5. Existing Geomorphology and Sediment Transport Conditions

The existing conditions geomorphology and sediment transport of the Klamath River from J.C. Boyle Reservoir to the Ocean are described to give context for the changes that may occur as the result of the No Action and Dam Removal Alternatives.

5.1. Geological Setting

The geomorphic provinces along the Klamath River have a diverse geologic history of formation and deformation. In the upper watershed, from the Klamath Basin headwaters to Iron Gate Dam, the Basin and Range and Modoc Plateau geomorphic provinces have a physiography with subdued relief, low gradient streams, broad basins and many lakes and marshes. The Basin and Range province consists of Miocene age basalts with high permeability and internally drained basins. The ranges are block-faulted with intervening down dropped basins typical of the Basin and Range province in other areas. The Modoc Plateau Province consists of thick sequences of tuffs and basalt flows that form a relatively flat tableland physiography in part of the province. The region was extensively faulted during the late Miocene, forming a series of mountain ranges. Drainage systems were also disrupted, creating lakes in between the ranges. Quaternary age shield volcanoes and cinder cones also are common on the landscape and younger than the extensive basalt flows.

The Lower Klamath Basin, from Iron Gate Dam to the Klamath River mouth, consists of metamorphic and plutonic rocks that have a complex history of metamorphism and volcanism. Geomorphic provinces include the Cascade Range, Klamath Mountains, and Northern Coast Ranges. The Cascade Range Province consists of the Western Cascade and High Cascade volcanics. The western cascade rocks were formed during uplift and folding during the late Eocene to Pliocene. They include lava flows and pyroclastics and in places interbedded nonmarine and shallow marine sedimentary rocks. The composition of most of the rocks is andesitic, but ranges from olivine basalt to rhyolite. They are underlain by Eocene sedimentary rocks of the Hornbrook Formation or by pre-Cretaceous plutonic and metamorphic basement rocks. The Cretaceous Hornbrook Formation has about a 5,000-ft thickness near the California-Oregon border in the Hornbrook area and consists of conglomerate, sandstone, and siltstone. The High Cascade Range rocks overlie the Western Cascade rocks and are part of a time period of renewed volcanism, in which early flows in the group produced wide spreading flows and small shield volcanoes and fissures, being more basaltic. Later flows became more siliceous in composition, and thus, were more explosive, building large peaks in the Cascade Range.

The Klamath Mountains Province consists of rocks uplifted during the Nevadan orogeny in Late Jurassic time. These rocks are more resistant to weathering, and thus, form a major change from low-relief terrain to high-relief terrain with prominent peaks and ridges along the Klamath River near Cottonwood Creek. Rocks range in age from Ordovician to Late Jurassic and form a series of arcuate belts that are defined on the basis of lithology and have varying degrees of metamorphism. They include the Eastern Klamath belt, central Metamorphic belt, Western Paleozoic and Triassic belt and the Western Jurassic belt. The belts developed as accreted terranes during tectonic episodes of subduction along the continental margin.

Near the mouth of the Klamath River is the Northern Coast Range, which consists of a thick sequence of Mesozoic and Cenozoic sedimentary rocks that were deformed during the Cenozoic. Along the Klamath River, rocks of the Franciscan Formation dominate the landscape and are composed of metasedimentary and metavolcanic rocks as well as mélange, which form a hummocky landscape due to its tendency to develop landslides.

5.2. Geomorphology

This section provides geomorphic information relevant to the proposed dam removal on the Klamath River. Tasks include: (1) to provide baseline geomorphic data prior to the proposed dam removal for Iron Gate Dam to Happy Camp, CA; and (2) to interpret the geomorphology within the Iron Gate, Copco and J.C. Boyle Reservoir areas to help inform drawdown modeling scenarios and channel evolution following the dam removal.

In the upper watershed, from the Klamath Basin headwaters to Cottonwood Creek, physiography can be described as mostly subdued relief, low gradient streams, broad basins and many lakes and marshes (California Geological Survey, 2002). Sediment delivery from these areas to the reservoirs is low, due to a sparse drainage network, limited surface runoff, and the trapping of sediment in the basins, lakes and marshes of the upper watershed (FERC, 2004b; Stillwater Sciences, 2010). Near Cottonwood Creek, the watershed transitions into the Klamath Mountains Province that consists of rocks more resistant to weathering which have formed high-relief terrain with prominent peaks. Sediment delivery to the Klamath River is higher within this terrain due to the steep drainages that are able to mobilize, transport, and deliver more sediment during storms to the main stem (FERC, 2004b; Figure 5-1).

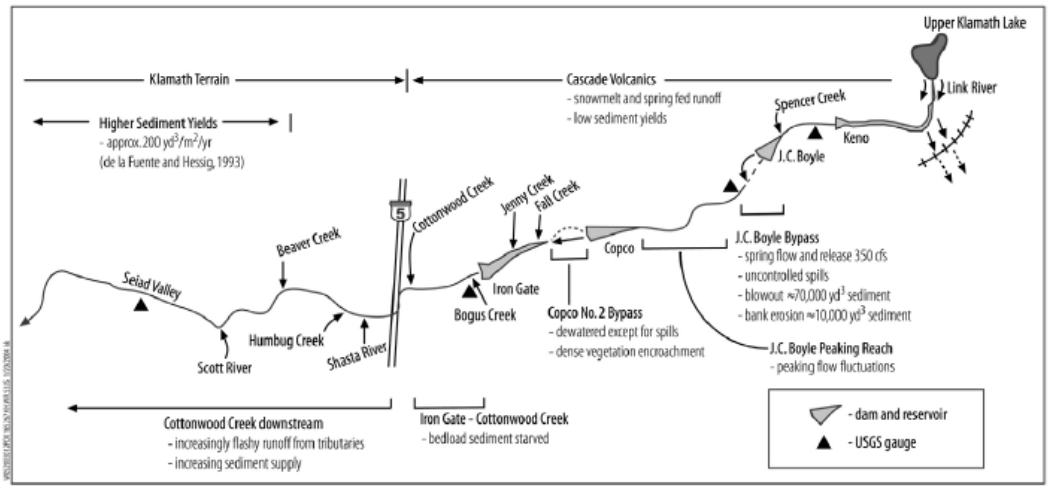

Figure 5-1. Reach Description from FERC (2004b).

5.2.1. DATA SOURCES

Several sources of existing data were used to develop geomorphic information for the study. Ayers (1999) produced geomorphic maps from the Klamath River estuary to Iron Gate Dam showing the extent of geomorphic features along the river corridor. Data from Happy Camp, CA to Iron Gate Dam were used most extensively and digitized in order to complement the extent of detailed modeling for the study. Rectified historical pre-dam aerial photography and topography were utilized from PacifiCorp, Inc., and JC Headwaters, Inc. (2002) to map pre-dam geomorphic features. These were compared to bathymetric data developed by JC Headwaters, Inc. (2002). Alluvial features mapped by CH2MHill as part of the FERC Fisheries Final Technical Report are also reviewed and discussed in the section, although they are not directly comparable to the geomorphic information developed in this study (PacifiCorp, 2004). PWA, Ltd. (2009) provided geomorphic descriptions of the pre-dam geomorphology and habitat, mostly related to the river channel and riparian vegetation. Information related to reservoir slope stability is also used in this section and was developed by PanGeo, Inc. as part of the PWA (2009) study.

The detailed geomorphic maps are located in Appendix H. Geomorphic Mapping.

5.2.2. DOWNSTREAM OF IRON GATE DAM

During 1997, Ayers (1999) conducted field work to map and interpret geomorphic features along the Klamath River from Iron Gate Dam to the Klamath River estuary. During the course of the study, features including unvegetated bars, floodplain, vegetated bars, stream terraces, landslides, bedrock, and tributary alluvial fans were mapped and described for each reach. Maps, produced for the USFWS, were not available and, therefore, were recreated in digital form for this study for the reach from Iron Gate Dam to Happy Camp, CA. To complete this task, the original draft mapping by Ayers (1999) was digitized using the USGS

7.5' topographic maps and digital terrain data produced by Woolpert, Inc. An initial reconnaissance was also conducted for this study reach to review the Ayers geomorphic mapping and determine if any features had changed along the river since the 1999 field mapping. Descriptions of the reach from Happy Camp, CA to the Klamath River estuary are derived entirely from Ayers work; field reconnaissance was not performed for this reach. Maps are provided in the Geo_Spatial Base Map Data Dictionary for this project (Reclamation, 2010b). Features depicted on the geomorphic maps are described below in sections 5.2.2.1 through 5.2.2.6. The reaches are shown Figure 5-2.

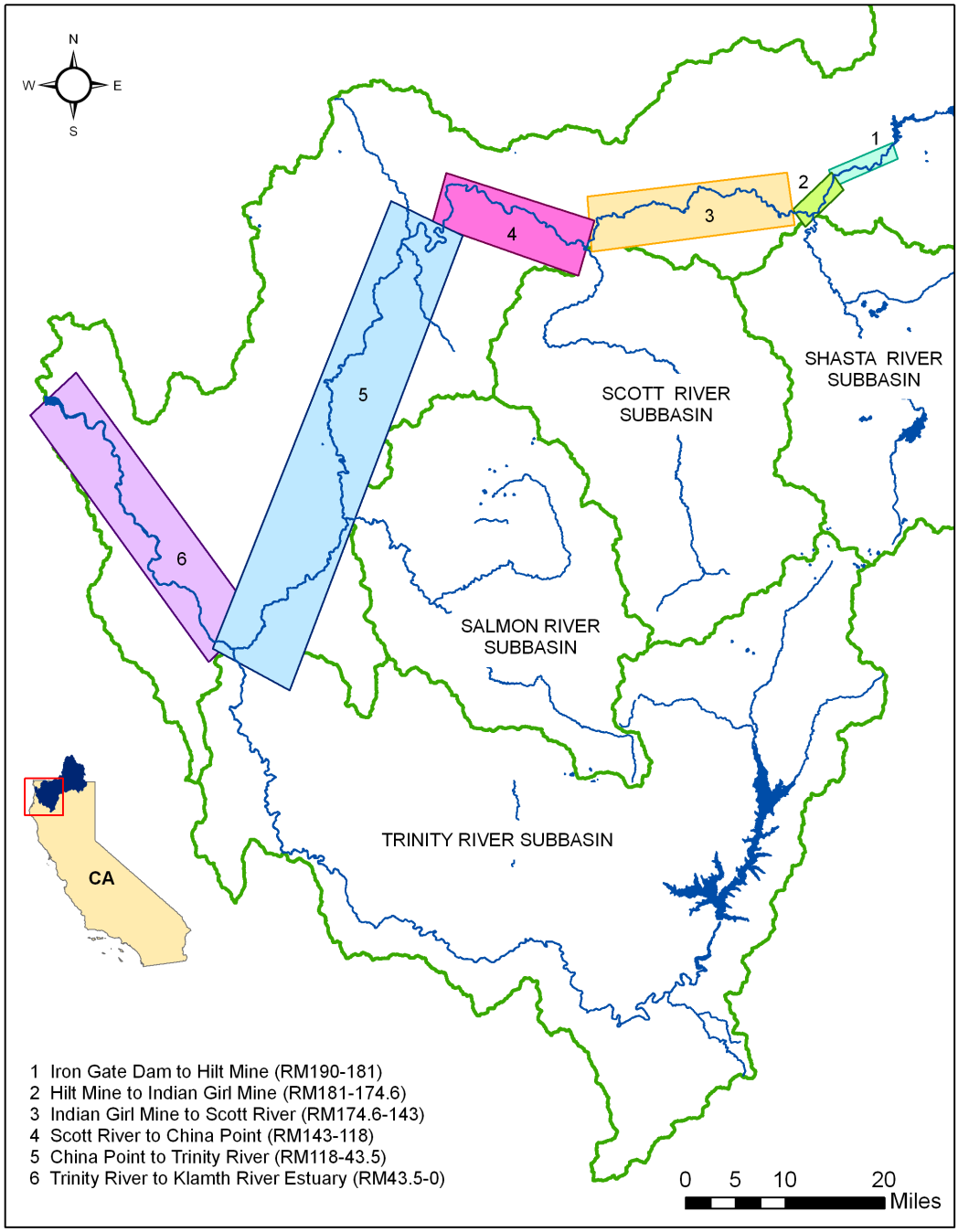

Figure 5-2. Map of Geomorphic Reaches.

5.2.2.1. Iron Gate Dam to Hilt Mine (USGS RM 181-190)

The first reach downstream from Iron Gate Dam consists of a narrow floodplain and terraces confined by bedrock hills of the Western Cascade Volcanics and sedimentary rocks of the Cretaceous Hornbrook Formation. The channel is mostly single thread with a few areas of split flow that form mid-channel bars and side channels of short length. Most of the bars are at least partially vegetated, leaving few areas of exposed bars in the reach. Main tributaries that enter the reach include Brush Creek, Bogus Creek, Little Bogus Creek, Willow Creek, and Cottonwood Creek. These tributaries form alluvial fans at their confluence with the Klamath River, which are all relatively small in area with the exception of Cottonwood Creek, which forms a large alluvial fan and terraces related to the tributary. Klamath River terraces are carved into the Cottonwood Creek alluvial fan deposits, suggesting that sediment input from Cottonwood Creek is limited to areas near and within the main channel of Cottonwood Creek.

5.2.2.2. Indian Girl Mine to Hilt Mine (USGS RM 174.6-181)

In this reach, the change in bedrock lithology marks a transition in channel confinement where the more resistant metasedimentary and metavolcaniclastic rocks of the Western Paleozoic and Triassic belt create a narrow canyon with narrow alternating terraces along the reach length. Few bars exist in this reach; at RM 179, a mid-channel bar appears to be associated with the Williams Creek alluvial fan, which enters at the upstream end of the high terrace of the Randolf Collier rest area. The Shasta River enters from the south near RM 177 and forms a small gravel bar at its confluence with the Klamath River. The lack of a large alluvial fan at the confluence or formation of bars downstream of the confluence indicates a limited coarse sediment supply from the Shasta River.

Ayers (1999) notes, however, that the supply of suspended sediment could be substantial. The only other notable tributary in the reach is Ash Creek, which forms a fan of negligible size at its confluence with the Klamath River. Ayers also notes many features associated with in stream mining, including low cobble-boulder benches and bars and a few wing-dam pits.

5.2.2.3. Scott River to Indian Girl Mine (USGS RM 143-174.6)

From Indian Girl Mine, the river valley broadens slightly within the canyon and allows for the preservation of broad, gravelly terraces that have been extensively mined. In areas not obscured by mining, overflow channels can be observed on the terrace surfaces. Unvegetated bars are more prevalent in this reach and exist as point bars along the inside bends of channel meanders as well as mid-channel bar

and side channel complexes. The channel maintains a mostly single thread meandering morphology with some areas of split flow around mid-channel bars.

At Gottville, CA, several tributaries enter from the north and form a large alluvial fan complex that constricts the river and forms the Langley Falls rapid and associated large eddy directly upstream.

Downstream of Gottville, CA from RM 166 to 161.5, the river valley narrows to about half the width of that upstream and flows through ultramafic rocks of the Cretaceous Franciscan complex. Low terraces and point bars exist in this reach and have been extensively mined with tailings piles still visible on some of the surfaces. Channel morphology is less sinuous than that upstream and is single thread with a few small mid-channel bars. At the downstream end of this subreach, the Miller Gulch alluvial fan constricts the channel, forming an eddy between the upstream end of the Miller Gulch fan and a small tributary fan from the opposite bank.

From Miller Gulch (RM 161.5) to Horse Creek (near RM 147), the river valley broadens again to include terraces with at least two levels and gravel bars. In several locations, the channel pattern increases in sinuosity, which is closely related to large alluvial fans that force the channel to the opposite bank and form split flow around large alluvial bars. A narrow section exists in this reach from about RM154 to 150 and is confined by bedrock on both sides of the river or by the Kohl Creek alluvial fan near RM152. A few lateral bars exist in this reach; however, most are too small to be mapped. From RM150 to Horse Creek, the river returns to a broader valley with a large paleochannel in the Cherry Flat area that has been extensively placer mined.

From Horse Creek to Scott River (near RM 147 to 143), the river valley narrows and is confined by bedrock on both sides of the river. Terraces and bars are restricted to the insides of meander bends. Several small tributaries enter in this reach, forming steep alluvial fans at the confluence with the Klamath River, some of which have narrow terraces cut on their front edges. Channel morphology is single thread with a few small unvegetated mid-channel bars and point bars.

In this reach, major tributaries that provide sediment to the Klamath River include Horse Creek, Beaver Creek, Lumgrey Creek, Empire Creek, Dutch Creek, and Humbug Creek. Other minor tributaries include Sambo Gulch, Barkhouse Creek and Little Humbug Creek.

5.2.2.4. Scott River to China Point (USGS RM 118-143)

Downstream of Scott River from RM 143 to 132, the extent and height of unvegetated gravel bars increases and bars become more prevalent with discontinuous narrow alluvial terraces forming along the canyon margins. Large alluvial fans control river position from RM 141 to 139 along the south side of the

river; sediment for these fans is generated from the Slinkard pluton, which are highly erodible plutonic rocks.

At Seiad Valley, large alluvial fans from Seiad Creek, Little Grider Creek, and Grider Creek form a wider alluvial valley in which terraces are cut on the front edges of the fans and large bars and riffles are formed along the river channel as a result of tributary sediment contributions to the Klamath River. Ayers and Associates (1999) noted that sediment deposition was significant from Grider Creek during the 1997 storm event and may have been at least partially mobilized from 1987 burned areas in the Grider Creek watershed. The 1997 peak flow at Iron Gate Dam was 20,500 cfs and was 117,000 cfs at Seiad Valley. From RM 130 to 121.5, the Klamath River flows through a sinuous bedrock canyon with unvegetated bars located on the insides of meander bends. Strath terraces and bedrock cored bars are prevalent in this reach.

From RM 121.5 to China Point, the canyon narrows as it enters bedrock of the Jurassic Galice Formation. Bedrock benches form along the channel margins. At China Point, an extensive unvegetated gravel bar is located on the inside of the bend along with a higher alluvial terrace. On the south side of the river, a paleochannel is elevated above the present channel. Major sediment contributing tributaries in this reach include: Thompson, Fort Goff, Portugese, Grider, Walker, O'Neil, and Macks Creeks. The tributaries are designated as major sediment contributors based on their large fans and recent observations of sediment contributions during the 1997 storm event (Ayers and Associates, 1999).

5.2.2.5. China Point to Trinity River (USGS RM 118-43.5)

Reaches from China Point to the Klamath River Estuary were not field checked during the course of this investigation. Observations for these reaches are summarized from Ayers and Associates (1999), who conducted an extensive field investigation of these reaches.

From China Point to Deason Flat (RM 118-104), the channel is narrow with numerous strath terraces that have been extensively mined. Well developed bars and riffles are formed at tributary confluences and meander bends, and in some areas, are also identified as relict mining features. The lower 3 miles of this reach (RM 107-104) contains a greater number of unvegetated bars, which are formed by sediment inputs from Elk and Indian creeks and channel constrictions downstream of RM 104. Tributaries in this reach contain large Quaternary landslides, with Indian Creek watershed containing the most of any tributary.

From Deason Flat to Dutch Creek (RM 104-92), the Klamath River flows through a narrow bedrock canyon with low bedrock benches and gravelly veneers. A narrow, inner bedrock channel is carved below the benches. Interspersed in this reach are wider sections having small strath terraces, that have been extensively mined, and unvegetated gravel bars formed by flow expansion as the river exits

from more constricted reaches and backwater effects where the river again enters a more constricted reach. This reach also contains notable Quaternary landslides along the main stem, the largest of which is located on the west side of the river from RM 98.5 to 93. Major Sediment contributing tributaries include Independence and Clear Creeks -- both watersheds burned during the 1987 forest fire.

From Dutch Creek to Trinity River (RM92-43.5), the Klamath River is contained in a narrow bedrock canyon with intermittent alluvial reaches. This reach also includes the wider alluvial valley at Orleans (RM 58.5). Geomorphic features include strath terrace and bars, alluvial terraces and bars, bedrock benches and alluvial fans. Numerous Quaternary landslides are located along the river and interact with the river through sediment contributions and controlling channel position. This reach is the downstream limit of channel mining on the Klamath River. Major sediment contributing tributaries include: Salmon River, Trinity River, Bluff Creek, Camp Creek, and Ukonom Creek.

5.2.2.6. Trinity River to Klamath River Estuary (USGS RM 43.5-0)

From Trinity River to Cappell Flat (RM 43.5-35), a narrow bedrock canyon with few bars and no floodplain or terraces exists, and is primarily bedrock controlled. Landslides and alluvial fans are less common compared to upstream reaches, but locations still exist where these features have temporarily dammed the river based on remnant boulders in the channel and deposits on opposite banks.

From Cappell Flat to Starwein Flat (RM 35-10), The Klamath River flows through a narrow, confined valley with minimal floodplain and terraces. Terraces that are mapped are formed at tributary confluences or behind large bars. The bars are well developed and are either alternate bars formed in straighter reaches or point bars formed at meander bends. The extent of the bars increases in the downstream direction. Tributaries may create split flow channels, mid-channel bars, and riffles at their confluences with the main stem. Major sediment contributing tributaries include: Blue, Pecwan, Cappell, Bear, and Tectah Creeks.

From Starwein Flat to the mouth (RM10-0), the river transitions into a wide valley with floodplain surfaces and narrow terrace remnants. Well developed bars of variable height are located along the reach; several large pools and few riffles are formed in this reach. Turwar Creek is the only major sediment producer in this reach, contributing mostly fines to the Klamath River.

The Klamath River mouth experiences frequent flooding and has a spit formed across its mouth that is destroyed during floods and reformed by sediment reworking following floods. Ayers and Associates (1999) document several historical accounts that describe conditions similar to present day at the Klamath River mouth, which leads Ayers to conclude that present sediment deposition is similar to deposition during early settlement (mid-1880’s).

5.2.3. COMPARISONS TO PREVIOUS GEOMORPHIC MAPPING

Based on reconnaissance from Iron Gate to Happy Camp on the Klamath River, channel changes since 1999 along the road have been minor. Lateral channel positions have remained very similar due to the bedrock control that is prevalent throughout the Klamath River downstream of Iron Gate Dam. Bars have remained in similar locations for the most part since the channel mapping in 1999. Through historical photo analysis, Ayers (1999) observed that even over the historical period, channel changes were minimal and channel bars remained in similar locations. During the course of our field reconnaissance in 2009, most of the changes since 1999 are in the amount of vegetation on gravel bars. In 1999, Ayers described many bars as unvegetated while in 2009 these bars have young willows established on their surfaces. It is likely that in 1999, the bars had been recently scoured by the 1997 flood and had remained relatively vegetation free for the 1999 field work. A few areas had bars that had reduced in size or that had lost small side channels following bar attachment to stream banks or where multiple mid-channel bars had coalesced. A few other areas were modified in Ayers mapping based on field observations. For example, near RM155 and 156, an additional terrace was added to the mapping, splitting Ayers single terrace into 2 terraces.

Table 5-1. Changes made to Ayers (1999) mapping based on 2009-10 field observations and aerial photography

River mile	Description of changes
185	Added vegetated bar on right bank
184-183	Unvegetated bar is now vegetated
182-181	Unvegetated bar is now vegetated with young trees
181	Osburger Gulch: added small terrace cut on alluvial fan edge
173-172	Unvegetated bars are now vegetated
172-171	Humbug Creek: changed terrace to large bar
171-170	Some side channels filled in with islands attached to banks
169	Unvegetated bar has grown laterally
167	Low bar is only located along inside bend as a point bar, does not extend along slope in a narrow strip
164-163	Unvegetated bar is now vegetated
158-157	Island along left branch just downstream of split flow is gone
157	Bar on right bank is now vegetated
156	Bars are now vegetated with willows
156-155	Two terraces mapped on left bank rather than one
154	Extended bar on right bank further toward road
153	Unvegetated bar is now vegetated
151-150	Unvegetated bars are now vegetated
150	Split flow is gone, bar is now attached to bank and vegetated
147	New island developed
146	New island developed
146-145	Bars are now vegetated with willows
144	Clipped fan toe is now vegetated
143	More bars are unvegetated

River mile	Description of changes
142-141	Unvegetated bars are vegetated with willows
138-137	Island merged with point bar to form a single bar; side channel is filled in
135-134	Unvegetated bar has decreased in size
133	Uvegetated bar is now vegetated along left bank
133-132	Island downstream of Seiad Bridge has increased in size
131-130	Modified terrace mapping based on LiDAR
130	Island decreased in size since 1999
128	Bar is now vegetated with willows
127	Weak side channel and island developed since 1999
127-126	Bar near Fort Goff Creek is now vegetated with willows
125	Unvegetated bar is now vegetated
122	Small bar is now vegetated
118-117	Small island mapped in 1999 along left bank across from China Point is not present, other nearby bars remain unvegetated
109-108	Bar is now vegetated with willows
107	Portion of low bar on right bank is now vegetated

Alluvial features were mapped by CH2MHill from Iron Gate Dam to Seiad Valley. The alluvial areas correspond to areas that were observed to have little vegetation or linear alignments of young vegetation and scoured surfaces or clean sand, gravel and cobbles, indicating recent fluvial modification. These areas had to be located within the 2 to 5 year stage of flow events along the river. Submerged bars were also included in the mapped alluvial features when observed. The alluvial features mapped by CH2MHill and areas mapped as unvegetated bars in this study have similar extents in many locations from Iron Gate Dam to Seiad Valley. Some of CH2MHill's alluvial features are also mapped on Ayers (1999) terraces in places where the terraces are unvegetated or have young vegetation. Submerged bars were not mapped in this study; such that, none of CH2MHill's submerged alluvial features are included within the river channel mapping.

5.2.4. COPCO RESERVOIR HIGH POOL TO OREGON-CALIFORNIA STATE LINE

The mapped reach extends from RM 203 at the high pool of Copco Reservoir to RM 209 near the Oregon-California state line. Geomorphic surfaces were mapped in this reach in order to provide an analog to geomorphic surfaces that are currently inundated by the reservoirs. Channel planform is single thread with split flow around vegetated islands. The channel has a low sinuosity and is almost straight in some sections within this reach. Floodplain areas are about 2-5 feet above the channel and have irregular topography with grassy vegetation and some woody riparian vegetation. These surfaces typically have a dark brown soil that is mostly fine-grained with sandy and silty sediments (Figure 5-3; Figure 5-5). The most extensive surfaces within this reach are stream terraces adjacent to the channel. Terraces are grouped into younger and older map units. The younger terraces are about 5-10 feet above the channel with grasses and shrubs and relict

channels or overflow channels on their surfaces (Figure 5-4). Soils have a dark brown sandy surface horizon while subsurface horizons are sandy with rounded pebbles and cobbles. The older terraces are about 15-20 feet above the modern channel and may have pines and other grasses on their surfaces. From soils that were observable, these surfaces also have dark brown soils with rounded cobbles and occasional boulders. Due to the narrowness of the valley, the terraces typically alternate as the channel traverses from side to side across the north-south trending valley. Klamath Hot Springs, near RM 206, is located along the east side of the Klamath River and forms a wetland area on the low terrace surface. Other springs are noted on the hillsides of the USGS 7.5’ topographic map.

Figure 5-3. Examples of geomorphic surfaces in reach from Copco high pool to Oregon-California state line; a) floodplain surface and b) younger terrace.

Alluvial fans from small drainages issue from the hillsides and deposit on the surfaces of many of the terraces in the reach; but the fans are located too far from the channel to contribute any significant amounts sediment to the river or to exert control on river morphology. Alluvial fans from larger drainages form more expansive deposits that extend to the river channel contributing sediment to the channel through debris flows and erosion by the Klamath River. There are also larger alluvial fan and terrace remnants that are about 40-50 feet above the channel and have been isolated from channel processes for thousands of years. These surfaces are largely vegetated by oaks and are composed of large cobbles and boulders. Steep scarps are formed along their margins. Debris flow processes are still active on the surfaces of these features, delivering sediment from hill slopes during intense rainstorms. In a few areas, channels are incised into these surfaces to the Klamath River, but for the most part the sediment is deposited in the upper part of the surfaces.

The major tributaries that enter this reach include Long Prairie Creek, Edge Creek, and Shovel Creek. Long Prairie Creek and Edge Creek enter from the north, and drop steeply into the Klamath River canyon to form alluvial fans at their confluence with the Klamath River. Shovel Creek is a larger, lower gradient drainage with a wide floodplain, riparian corridor, and multiple channels near the confluence with Klamath River. When stream terraces or alluvial fans are absent, the Klamath River flows against bedrock of the Western Cascade volcanic. Hill slopes are sparsely vegetated and have colluvial deposits that have formed on slopes.

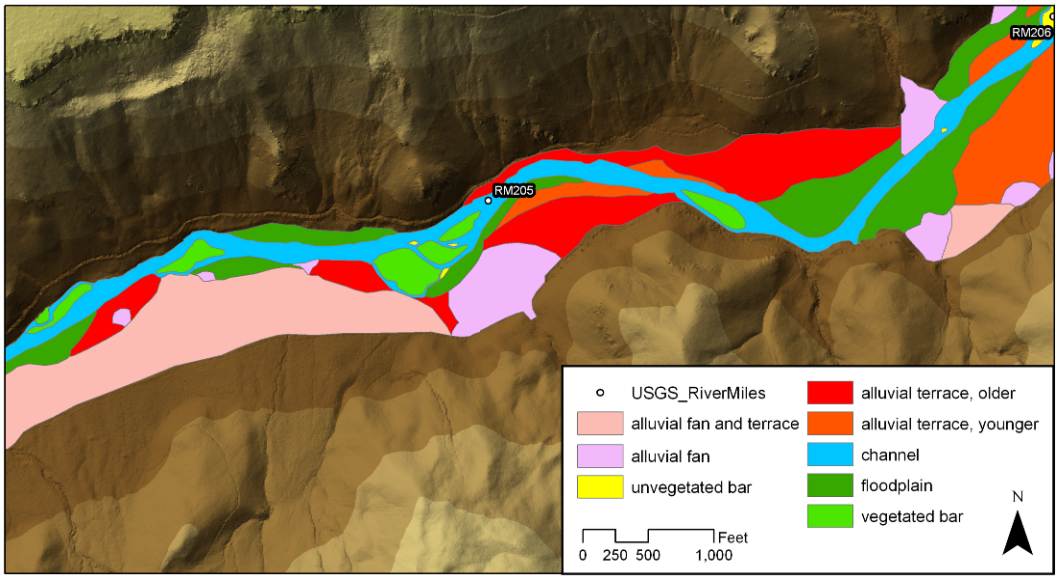

Figure 5-4. Example of mapping in the Copco analog reach from RM 203 to 209

Figure 5-5. Map unit descriptions, Copco Reservoir high pool to California-Oregon state line (RM 203-209)

Description	Map unit	Landscape Position	Materials
Channel	Qa3	same	Sand and cobbles
Unvegetated bar	Qa2	Adjacent to channel	Sand and cobbles
Vegetated bar	Qa1b	Adjacent to channel	Sand, silt and cobbles
floodplain	Qa1a	2-5 ft above channel	Sand and silt
Alluvial terrace, younger	Qt2	5-10 ft above channel	Sand, silt and cobbles
Alluvial terrace, older	Qt1	15-20 ft above channel	Sand, silt and cobbles
Alluvial fan	Qaf	Adjacent to hill slope, may or may not extend to river channel; height above channel varies	Cobbles and boulders in a sandy matrix
Alluvial fan and terrace	Qaf/Qt	Extends from hill slope to channel; height above channel varies	Ranges from cobbles and boulders in a sandy matrix to cobbly sand and silt

5.2.5. RESERVOIR AREAS

Geomorphology of the reservoir areas is delineated based on historical aerial photography and topographic maps that were rectified by Pacificorp (2004) and Eilers and Gubala, Inc (2003).

5.2.5.1. J.C. Boyle Reservoir

At J.C. Boyle Reservoir, pre-dam aerial photography from 1952 shows a flow expansion zone at the upper end of the reservoir where the river exits from a steep, narrow canyon with multiple rapids or riffles visible on the aerial photography. The river flows west, and then turns abruptly to the south as it encounters bedrock and alluvial fan deposits from an unnamed tributary. A large pool is formed at this location and remains in the bathymetric data collected in the reservoir area. Channel morphology was mostly single thread, with an area of split flow around a semi-vegetated island upstream of the Highway 21 Bridge and a few small side channels in the reach (Figure 5-6). From RM 228 to 226, the river corridor is wide enough to preserve some alluvial surfaces. Spencer Creek enters from the north and forms a large alluvial fan that extends to the river channel with, perhaps, a narrow floodplain surface cut on its edge. The tributary channel was multi-threaded in 1952 and probably supported wetland environments near its confluence with Klamath River. Downstream of Spencer Creek, extensive terrace surfaces less than 5 feet above the river channel were located on the left and right banks. Portions of these surfaces may be unvegetated bars that were modified frequently during larger peak discharges; however, the surfaces appear to be modified in 1952 photography and could not be delineated.

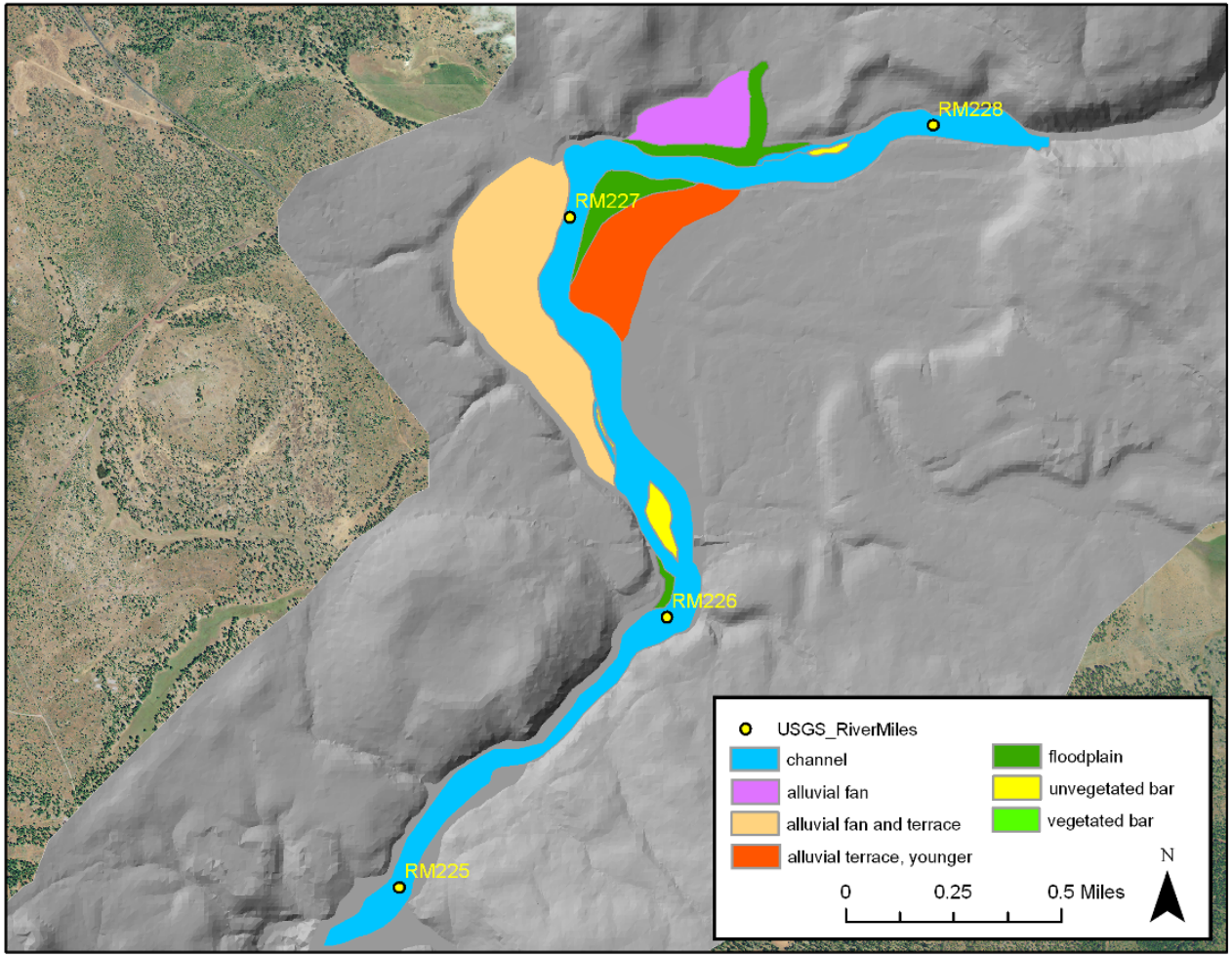

Figure 5-6. Geomorphic map of J.C. Boyle Reservoir.

5.2.5.1. Copco

Pre-dam geomorphology was interpreted using historical topographic maps of the reservoir area that were developed prior to inundation. The historical channel through Copco Reservoir consisted of asymmetrical meanders, controlled by bedrock on the outer bends. Deep pools were probably located in these bends; a couple of pools can still be observed in bathymetric data in the SW1/4 of section 27 and in the NW1/4 of section 35. In the upper portion of the reservoir from the high pool to about USGS RM 200, the channel was a mostly single-thread, sinuous channel with broad asymmetrical meanders. Terraces were located along most of the reach, and were mostly 5-10 feet above the river channel, which would correspond to the younger terrace in reaches mapped outside of the reservoir areas. In addition, there were areas designated with willow and brush vegetation, which could correspond to either floodplain areas or young alluvial terraces.

Downstream of RM 200 to about RM 199, the channel is more sinuous, perhaps due to the canyon constriction which begins near Copco 1 Dam. In this location, pyroclastic flows blocked the drainage, forming an ancient lake in the vicinity of Copco Reservoir. In this reach, the channel contained a greater number of vegetated islands, some abandoned channel meanders, and wetland or floodplain environments. Most surfaces in the reach were less than 5 feet above the river channel based on historical topography. A few terraces of 5-10 feet and 15-20 feet also exist in the reach, but are more limited in extent. A notable paleochannel, which was abandoned by the Klamath River prior to the historical period, is now partially occupied by Beaver Creek that enters Klamath River from the north. Downstream of RM 199 to the high pool of Iron Gate Reservoir, the Klamath River enters a narrow canyon incised into the pyroclastic deposits of the High Cascade Volcanics; only a few narrow terraces exist in this reach.

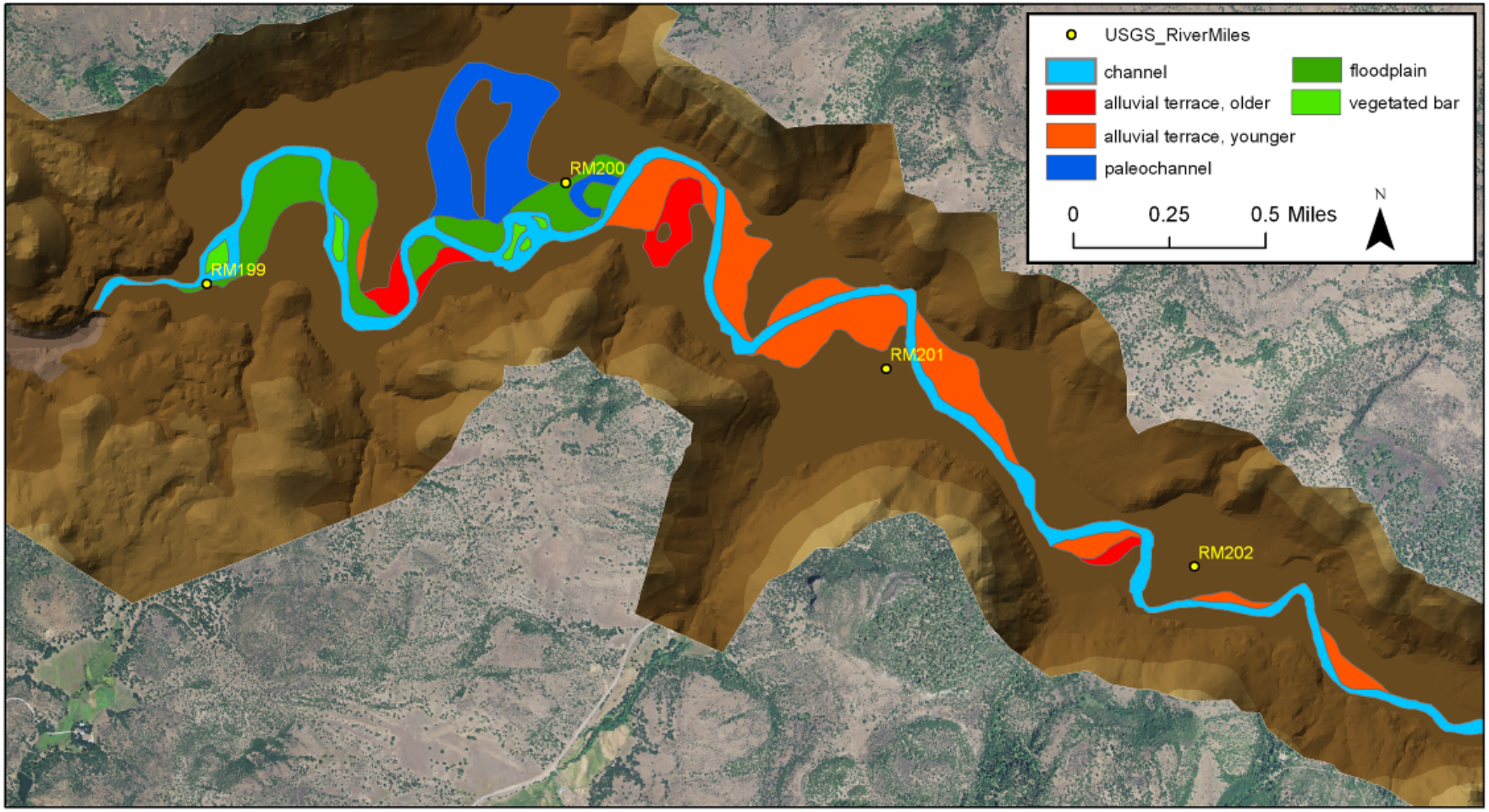

Figure 5-7. Geomorphic map of Copco Reservoir.

5.2.5.2. Iron Gate

The reach of the Klamath River through Iron Gate Reservoir consists of a confined bedrock canyon formed in andesite of the Western Cascade Volcanics. Based on 1955 aerial photography and pre-dam topography, terraces were located along the insides of meander bends and near tributary confluences and were typically less than 10 feet above the river channel based on the 10ft contours on the topographic map (Figure 5-8). These surfaces would correspond to younger terraces mapped in adjacent reaches without reservoirs and therefore would consist of an organic-rich, sandy surface horizon with gravelly materials below the surface horizon. Tributaries along this reach had mostly minor alluvial fans at their confluences with the Klamath River, likely indicating that the Klamath River was readily able to erode material in the main channel deposited by tributaries. A few alluvial fans exist that controlled the historical river position along this reach, but these are limited in extent.

Historical channel morphology is single thread with uncommon split flow areas and vegetated islands. A few unvegetated gravel bars are also visible in the 1955 aerial photography. Channel constrictions are located near RM 195 and 196, where large pools are formed behind the narrowed channel. It is likely that bedrock was visible in at least part of the channel bed in these locations. The presence of visible riffles in 1955 aerial photography indicate steeper reaches with higher velocities from RM 194 to RM 192 and from RM 197 to RM 195. Other reaches such as from RM 192 to Iron Gate Dam have riffles located near tributaries or gulches that contribute large sediment to the river, but for the most part likely contained pools or lower velocity sections.

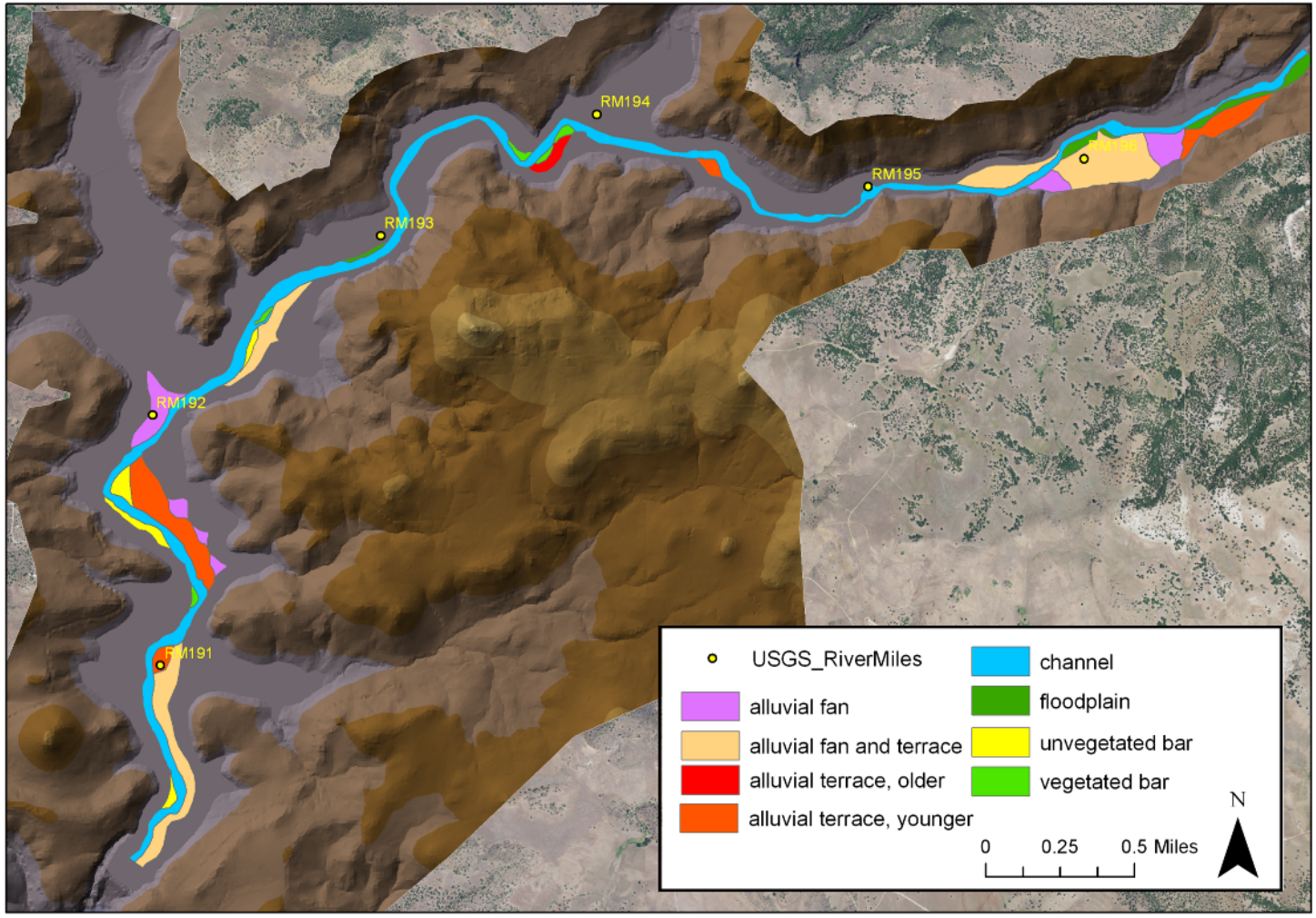

Figure 5-8. Geomorphic map of Iron Gate Reservoir.

5.2.6. HISTORICAL CHANNEL ALIGNMENTS VS. BATHYMETRIC DATA

Historical channel alignments were developed by Eilers and Gubala, Inc. from historical topographic maps of the reservoir areas. Comparison of the historical channel alignments with a hypothetical channel alignment following dam removal using bathymetric data was made to determine if there were any major changes to channel position from reservoir sedimentation or other effect. Comparisons at J.C. Boyle Reservoir and Iron Gate Reservoir revealed that there were no major changes between the low elevation points in the bathymetric data and historical channel position prior to dam construction. At Copco Reservoir, most of the channel alignments were similar with an exception in the vicinity of USGS RM 202 (Figure 5-9). The low elevations derived from bathymetric data at this location are in a much different location than the historical channel alignment. If the bathymetric data are correct, there may be some material that has slumped into the reservoir along the southern side, burying the location of the historical channel and shifting the low elevations to the north in the reservoir. In other locations within Copco Reservoir, bathymetric data and historical channel alignments match sedimentation.

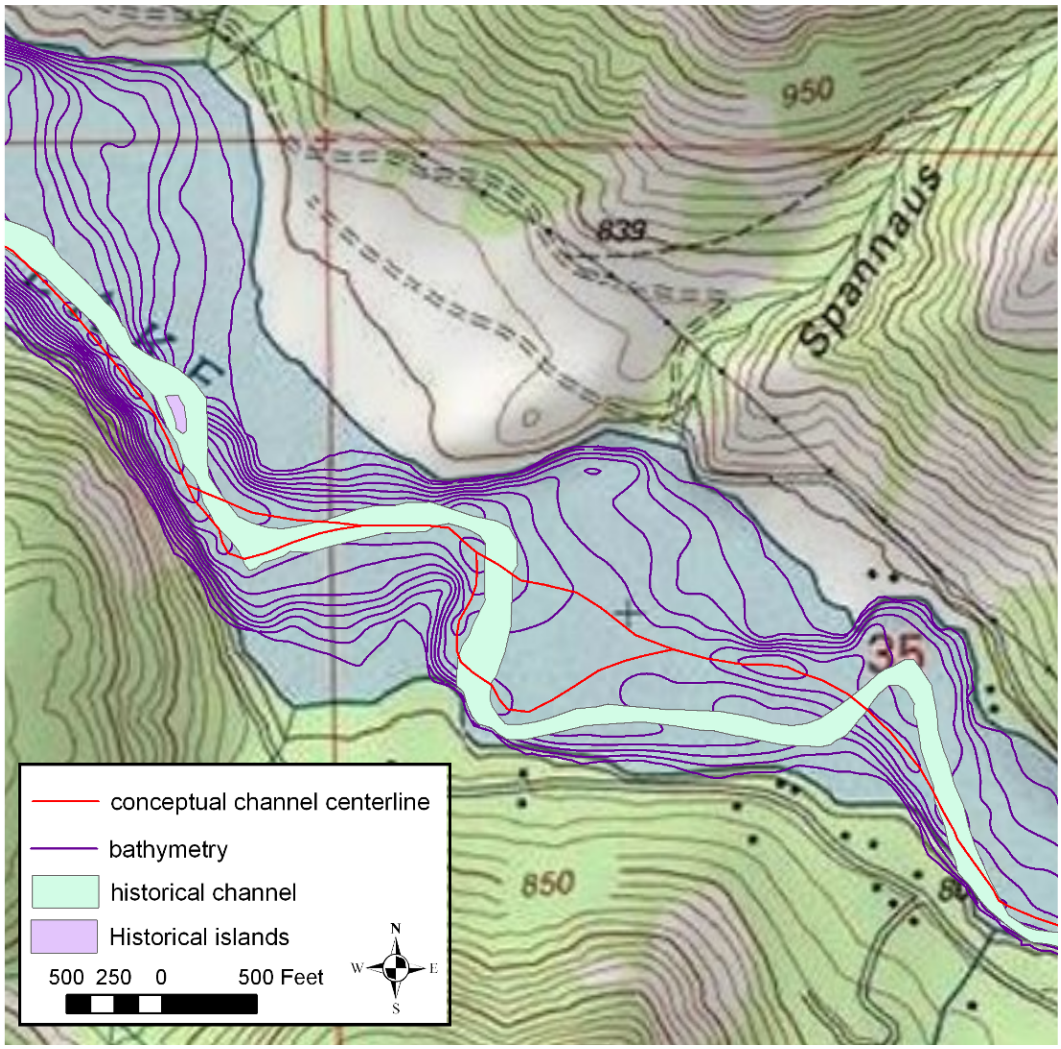

Figure 5-9. Comparison of historical channel alignment and bathymetric data near RM 202, Copco Reservoir.

5.2.7. COMPARISON TO VEGETATION RESTORATION MAPS USING BATHYMETRIC DATA

Geomorphic mapping is based on landform characteristics and the physical processes that created the landforms. Therefore, while the vegetation mapping and geomorphic mapping should be similar, some differences are to be expected. At Copco Reservoir, areas delineated as potential wetlands correspond to floodplain or young alluvial surfaces on the geomorphic map. Areas of active restoration may correspond to young alluvial terraces, but are also located on flat areas that are elevated above the pre-dam channel. Areas of passive restoration are located in upland areas or on older alluvial terraces. At Copco Reservoir, the large paleochannel mapped in the vicinity of Beaver Creek shows a wide variety of vegetation types due to changes in slope within the relict channel. Wetland vegetation is depicted in areas on the vegetation restoration map that are similarly located on the historical maps. These areas are mapped as part of the paleochannel landform, which can include wetland areas. In Iron Gate Reservoir, vegetation

restoration areas are limited to small areas of expansion within the confined canyon, mainly along the major tributaries, and areas along the main channel, mapped as terraces or a combination of alluvial fans and terraces. At J.C. Boyle Reservoir, potential riparian areas are limited to banks and narrow sections along the channel. These areas roughly correspond to geomorphic mapping of floodplain and young alluvial terraces. Most of the areas within the reservoir are classified on the vegetation restoration maps as upland. These areas are mapped as terraces or alluvial fans on the geomorphic map, or may be located outside of areas that were mapped.

5.3. Sediment loads

Stillwater Sciences (2010) summarized several studies analyzing sediment loads in the basin and their results are given in Table 5-2. They used several reports to develop tributary sediment supplies to the Klamath River from Iron Gate Dam all the way to the ocean. They divided the estimates into the total sediment supply and the sediment supply of sediment sizes greater than 0.063 mm.

Based upon the work of Stillwater Sciences (2010), only a small fraction of the sediment load is supplied to the Klamath River from the watershed above Keno Dam. Because of its large surface area, Upper Klamath Lake traps practically all sediment entering it from its tributaries. From Keno Dam to Iron Gate Dam, the average annual sediment delivery was estimated to be approximately 150,000 ton/yr. The Scott River supplies approximately 607,000 tons/yr, the Salmon 320,000 tons/yr and the Trinity 3,300,000 tons/yr. The total annual delivery of sediment to the ocean from the Klamath River was estimated to be 5,800,000 tons/yr. The total annual delivery of sediment with a particle size greater than 0.063 mm was estimated to be 1,800,000 tons/yr. These estimates were based upon a variety of studies and data sets collected over different time periods. The Stillwater Study ignored temporal trends in the sediment load.

Suspended sediment data was collected by the USGS at the USGS gage on the Shasta River near Yreka, and on the Klamath River at Orleans and Klamath. The data is presented in Figure 5-10, Figure 5-11, and Figure 5-12, respectively. The data collected at the Yreka gage was from 1957 to 1960, the Orleans gage was from 1957 to 1979, and the Klamath gage was from 1974 to 1995. A simple power function was fit to the data as follows:

$$C = aQ^b$$

where, C = Suspended Sediment Concentration in mg/l
Q = flow rate in cfs
a, b = constants

The sum of the absolute value of the predicted and measured data was minimized to determine the value of *a*. A value of *b* was assumed to be 1.5 based upon visual fitting the data. The computed coefficients are given in Table 5-3. The sediment concentration during a 10-year flood (163,000 cfs) on the Klamath River at Orleans would be about 2,000 mg/l. A 2-year flood at Orleans is about 60,000 cfs and would have a suspended sediment concentration of about 800 mg/l. The data show considerable scatter about the best-fit line. Sediment concentrations commonly exceed 1,000 mg/l at Orleans, even at flows as small as 20,000 cfs.

The data from the Klamath gage from 1974 - 1984 was compared against the data from 1985 – 1995. A separate regression was fit to the data from 1985 – 1995 and there is a reduction in the *a* coefficient from 1.45E-5 to 1.1E-5, a reduction of

24%. The reduction in sediment loads could be caused by changes in land use or practices and the gradual recovery of the watershed from hydraulic mining.

There are no high flow suspended sediment data collected upstream of the Orleans gage. There are only low flow measurements of total suspended solids (TSS) collected by PacifiCorp downstream of their dams. The data collected downstream of Keno Dam and upstream of J.C. Boyle Dam are presented in Figure 5-14 and Figure 5-15. All the data was collected at flows less than 2,100 cfs and all the TSS measurements except those collected near 2,000 cfs were below 15 mg/l. Additional data on Total Suspended Solids is available from PacifiCorp on their website at: http://www.pacificorp.com/es/hydro/hl/kr.html#, and a list of their sampling sites is given in Table 5-4.

Because there is little information on sediment concentrations at high flows, the TSC attempted to synthesize a relationship between flow and sediment concentrations based upon the mass of sediment deposited behind the dams. An estimate of the volume and weight of deposition in the 3 reservoirs is given in Table 5-15. There is about 3.6 million tons of deposition in the three reservoirs. The fraction of the silt and clay sized material that is trapped by the three reservoirs is unknown, but assuming a trapping efficiency, it is possible to estimate the sediment concentration versus flow relationships necessary to deposit the measured volume behind the three dams. A flow duration curve is constructed at Iron Gate Dam based upon the 1962 – 2009 period of deposition in the reservoirs. This period is chosen because all three reservoirs have been in place during this period. The weight of deposited sediment since 1962 is estimated to be about 2.6 million tons. If the exponent *b* is assumed in the relationship between SSC and flow, then it is possible to solve for the constant *a* so that the weight of incoming sediment equals the weight of sediment deposited in the reservoirs. The values of the constant *a* were determined assuming two different exponents (0.7 and 1.5), and two different trap efficiencies (0.5 and 1.0). The results are shown in Figure 5-16. A 2-year flood is about 6,000 cfs at Iron Gate and the sediment concentration at this flow is estimated to be between 50 and 100 mg/l. There is considerable uncertainty in developing sediment concentration relationships from deposition data, but the main point behind this exercise is to demonstrate the likelihood that sediment concentrations will be higher at higher flows. This is also evidenced in a picture of the Confluence of the Klamath and Shasta Rivers at flood stage in January 2006 (Figure 5-17). The water in the photograph is noticeably laden with sediment.

Table 5-2. Annual sediment loads from Table 10 or Stillwater Sciences (2010). CWE refers to the Cumulative Watershed Effects assessment of the US Forest Service.

Table 10. Estimated sediment delivery to the Klamath River from Keno Dam to the Pacific Ocean.

Source area	RM[9]	Source area (mi^2)	Cumulative delivery[10] (tons y^{-1})		
			Total	≥0.063 mm	<0.063 mm
Keno Dam To Iron Gate Dam[1]	192.7	660	151,000	24,160	126,840
Iron Gate Dam to Cottonwood Creek[2]	184.9	151	160,961	25,754	135,207
Cottonwood Creek[3]	184.9	99	175,560	30,426	145,135
Cottonwood Creek to Shasta River[2]	179.3	18	177,715	31,115	146,600
Shasta River[2]	179.3	516	199,259	38,009	161,250
Shasta River to Beaver Creek[3]	163.3	106	231,710	48,393	183,316
Beaver Creek[4]	163.3	109	279,869	63,804	216,065
Beaver Creek to Scott River[5]	145.1	154	373,073	93,630	279,443
Scott River[5]	145.1	814	980,393	287,972	692,421
Scott River to Grider Creek[5]	129.4	128	1,048,860	309,881	738,978
Grider Creek to Indian Creek[5]	108.4	105	1,099,934	326,225	773,709
Indian Creek[3]	108.4	135	1,173,246	349,685	823,561
Elk Creek[3]	107.1	95	1,211,930	362,064	849,866
Clear Creek[3]	100.1	111	1,253,972	375,517	878,454
Dillon Creek[3]	85.8	73	1,282,389	384,611	897,778
Indian Creek to Dillon Creek[3]	85.8	137	1,354,759	407,769	946,990
Dillon Creek to Salmon River[3]	66.5	109	1,440,282	435,137	1,005,146
Salmon River[3]	66.5	751	1,760,904	537,736	1,223,169
Salmon River to Camp Creek[7]	57.3	27	1,785,769	545,693	1,240,077
Camp Creek[6]	57.3	42	1,831,523	560,334	1,271,190
Camp Creek to Red Cap Creek[7]	53.0	26	1,855,021	567,853	1,287,168
Red Cap Creek[6]	53.0	63	1,897,796	581,541	1,316,255
Red Cap Creek to Bluff Creek[7]	49.8	18	1,913,925	586,702	1,327,223
Bluff Creek[6]	49.8	74	2,014,594	618,916	1,395,678
Bluff Creek to Trinity River[7]	43.4	23	2,035,830	625,712	1,410,118
Trinity River[5]	43.4	2,274	5,353,164	1,687,259	3,665,905
Blue Creek[8]	16.1	125	5,455,971	1,720,157	3,735,814
Trinity River to Mouth[8]	0.0	367	5,834,091	1,841,155	3,992,936

1 Source: Reservoir sediment volumes reported in GEC 2006, sedimentation rates reported in Stillwater Sciences 2008.
2 Source: CWE analysis for Klamath National Forest lands (UDSA Forest Service 2004). Delivery from remaining areas extrapolated based on CWE modeled sediment delivery rates in similar terrain. Excludes source areas upstream of Dwinnell Reservoir and other disconnected areas in Shasta Valley.
3 Source: CWE analysis for Klamath National Forest lands (UDSA Forest Service 2004).
4 Source: CWE analysis for Mt. Ashland Late-Successional Reserve Habitat Restoration and Fuels Reduction Project (Elder 2006).
5 Source: Sediment TMDLs (NCRWQCB 2005; EPA 1998, 2001). Excludes source areas upstream of Trinity Dam.
6 Delivery from Camp, Red Cap, and Bluff creeks extrapolated using unit-area delivery rates by geologic unit reported in the Lower Middle Klamath Watershed Analysis.
7 Source: Lower Middle Klamath Watershed Analysis (USDA Forest Service 2003).
8 Source: Extrapolated from sediment delivery rates for similar terrain in Hunter Creek reported in the Green Diamond Habitat Conservation Plan (Simpson Resource Company 2002) and in the South Fork Trinity River sediment TMDL (EPA 1998).
9 River miles reported here are derived from a recent high resolution streamline and may vary from those reported in the PacifiCorp sediment budget.
10 Density = 1.5 tons yd^{-3}. Mass reported in US short tons. Above Cottonwood Creek, assumes 16% of total load is ≥0.063 based on grains size distribution of reservoir sediment (GEC 2006). Below Cottonwood Creek, assumes 10% of total load is bedload and 24% of suspended load is sand ≥0.063 (CDBW and SCC 2002). Coarse sediment delivery to the Ocean is less than presented in this table when attrition by abrasion is considered.

Table 5-3. Coefficients fit to all historical suspended sediment data.

	Shasta River		Orleans		Klamath	
Coefficient	Total	Sand	Total	Sand	Total	Sand
a	2.12E-01	-	5.26E-05	1.32E-05	1.45E-05	5.0E-06
b	0.7	-	1.5	1.5	1.5	1.5

Table 5-4. Additional PacifiCorp water quality sampling sites.

Site ID	River Mile	Site Name
KR15750	156.00	Klamath River at Walker Road Bridge
KR17923	176.00	Klamath River at I-5 Rest Area
KR18423	184.23	Klamath River at Klamathon Bridge
KR18973	189.73	Klamath River Iron Gate Dam outflow
KR19019	190.19	Iron Gate Reservoir near Dam
KR19645	196.45	Klamath River below Copco 2 Powerhouse
KR19874	198.74	Copco Reservoir near Dam
KR20642	206.42	Klamath River above Shovel Creek
KR22040	220.40	Klamath River at bottom of bypass
KR22460	224.60	Klamath River below J.C. Boyle dam
KR22822	228.22	Klamath River above J.C. Boyle reservoir
KR23334	233.34	Klamath River below Keno Dam
KR23435	234.35	Keno Reservoir at Highway 66 bridge
KR25312	253.12	Mouth of Link River

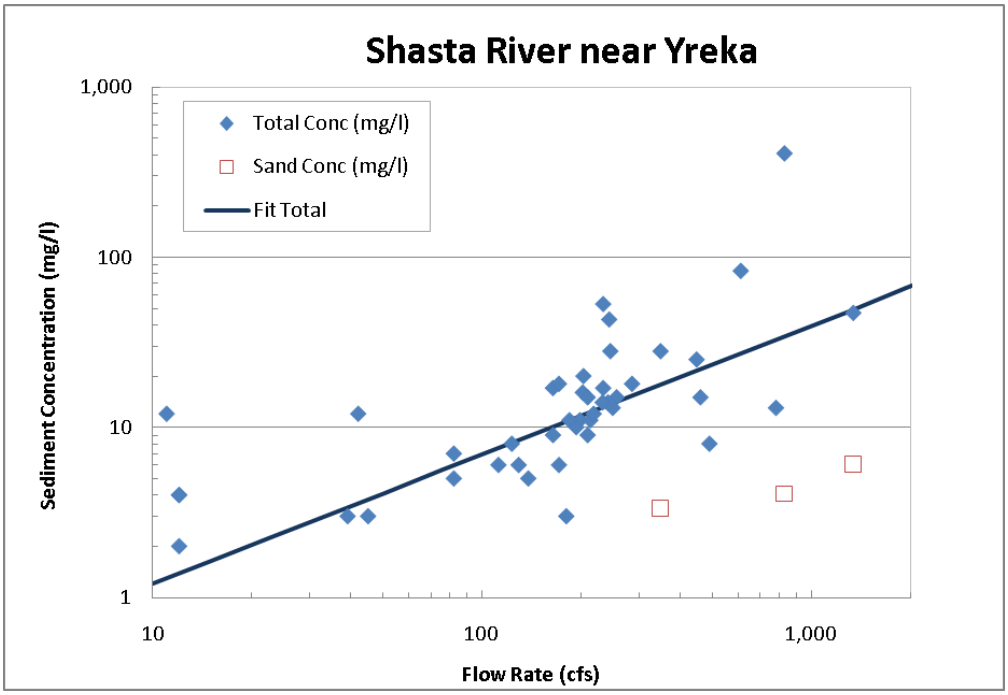

Figure 5-10. Suspended sediment data on Shasta River near Yreka.

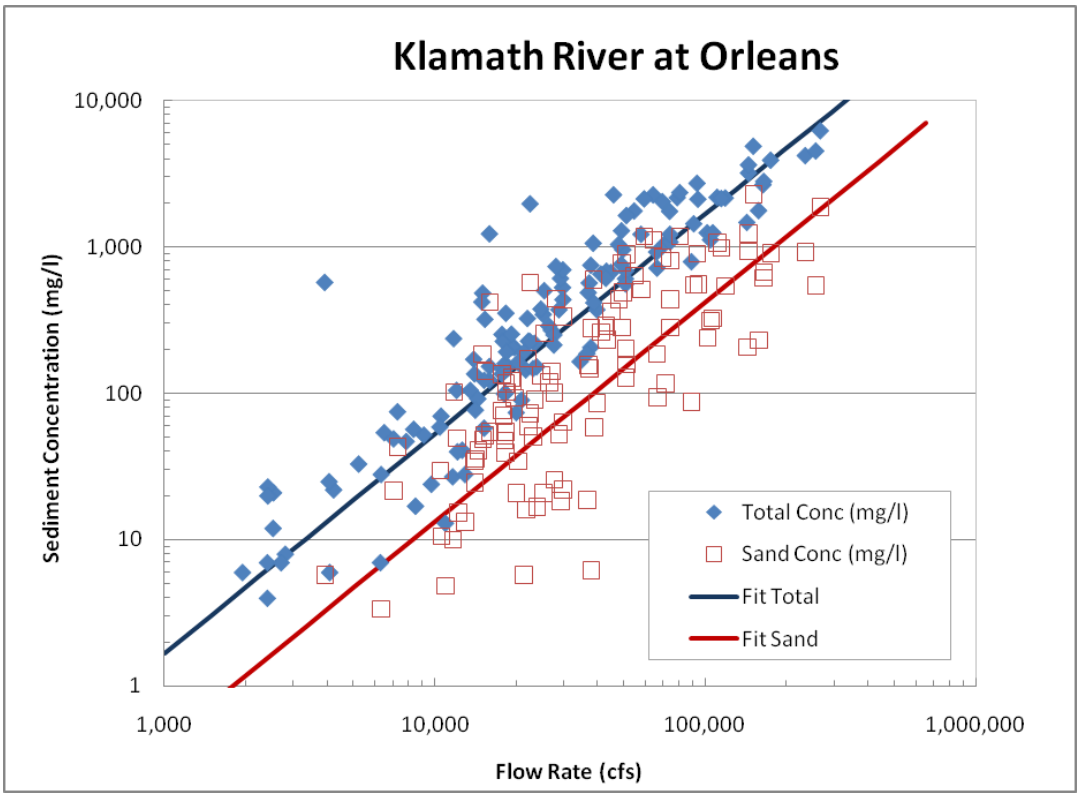

Figure 5-11. USGS Suspended sediment Data at Klamath River at Orleans.

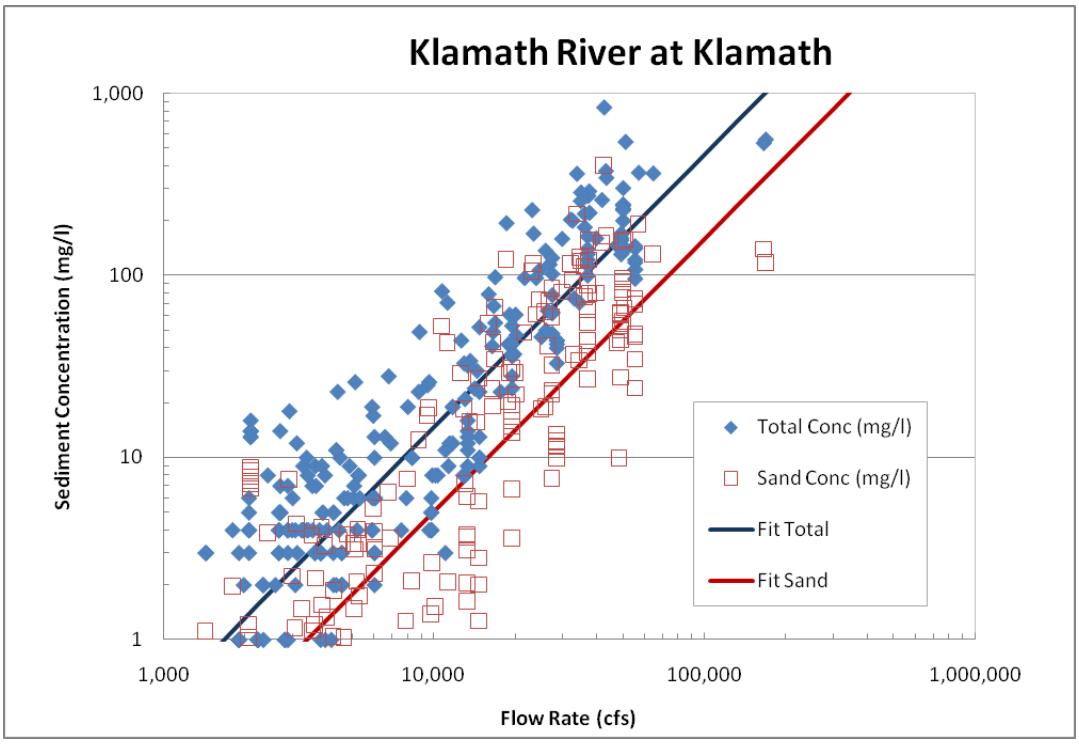

Figure 5-12. USGS Suspended sediment Data at Klamath River at Klamath.

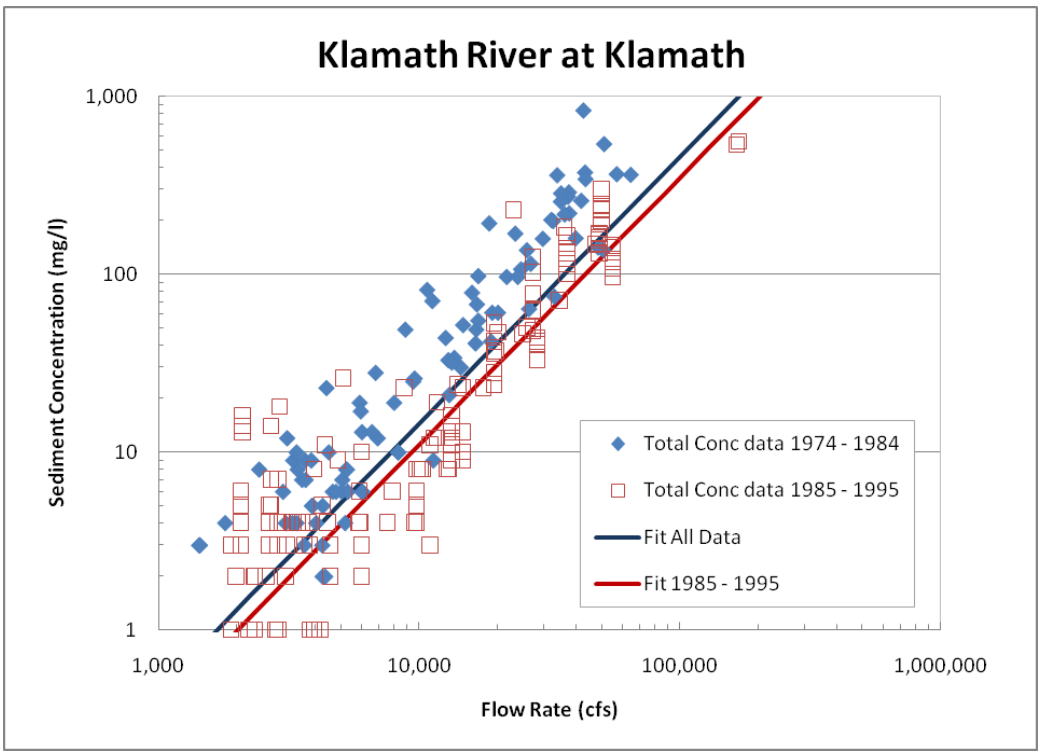

Figure 5-13. Comparison between rating curve fit to all data and that fit to data from 1985 to 1995.

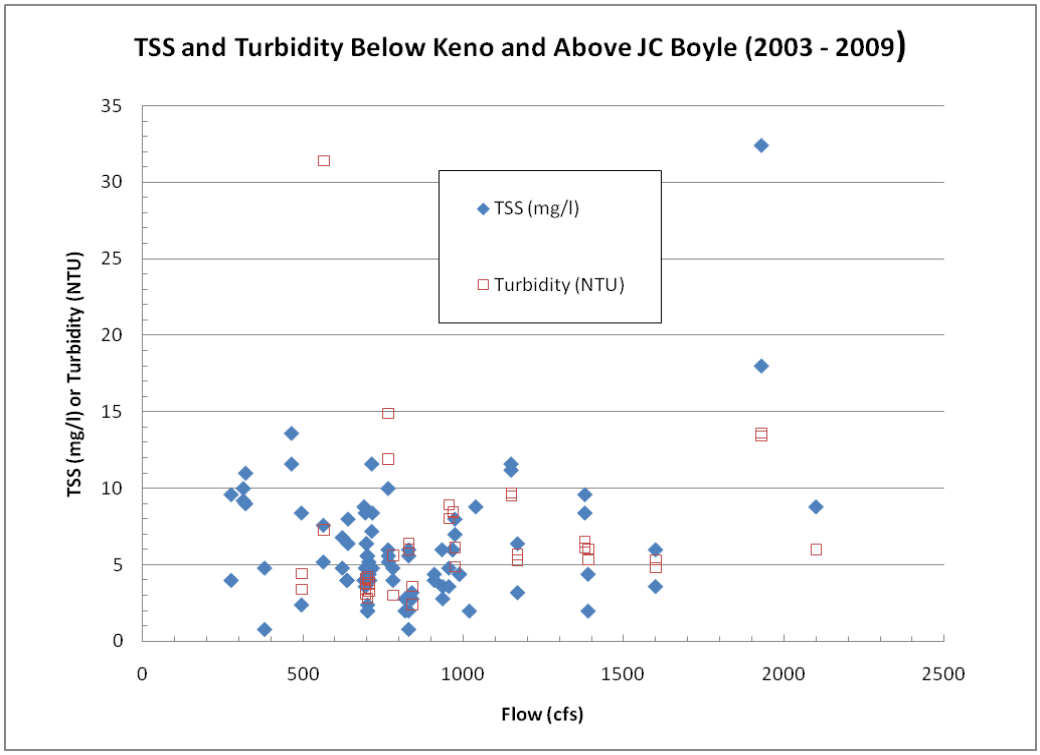

Figure 5-14. Total suspended solids (TSS) and turbidity data on Klamath River below Keno Dam and above J.C. Boyle Dam. Data collected by PacifiCorp from 2003 – 2009.

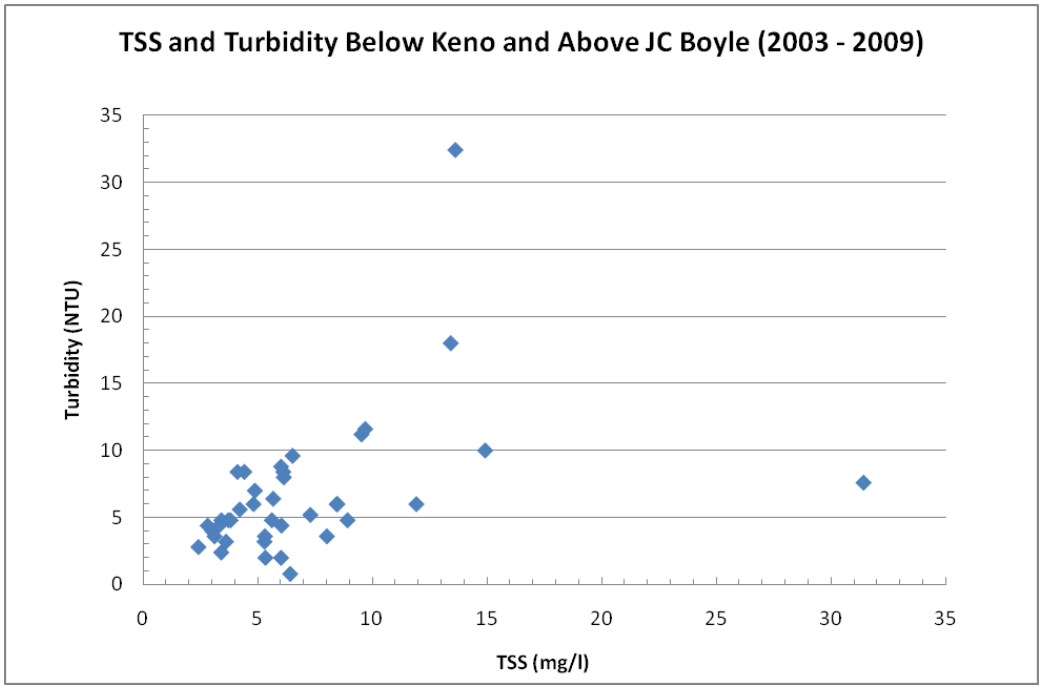

Figure 5-15. Relationship between suspended solids data and turbidity on Klamath River below Keno Dam and above J.C. Boyle Dam. Data collected by PacifiCorp from 2003 – 2009.

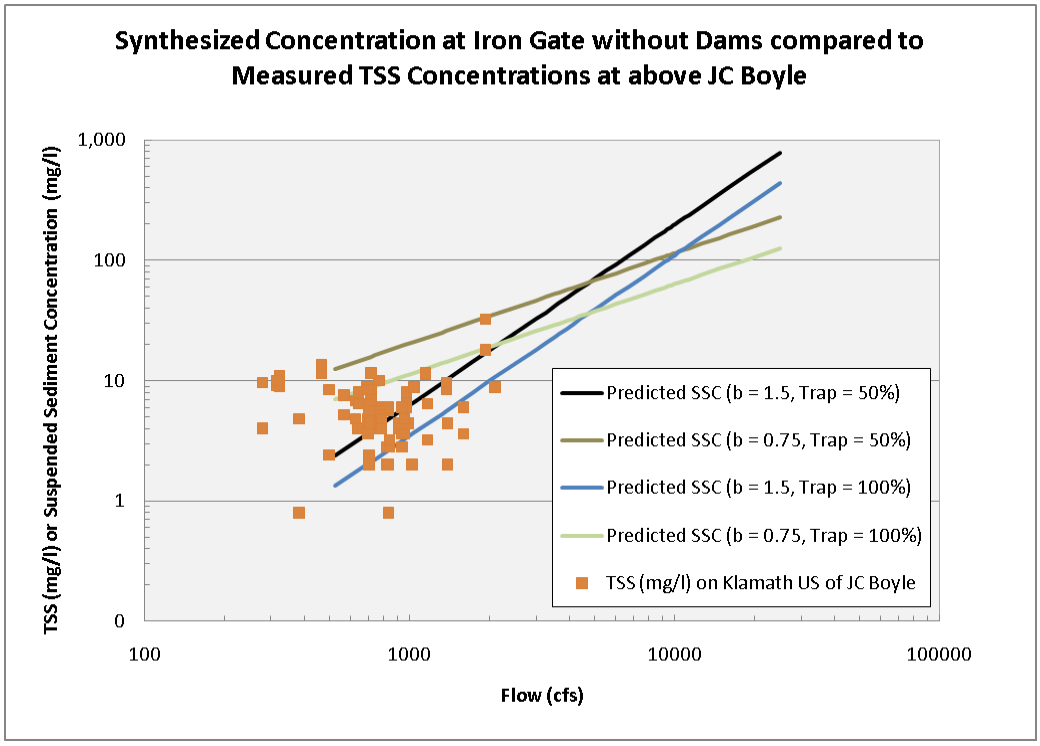

Figure 5-16. Sediment concentrations at Iron Gate synthesized from reservoir sedimentation rates.

Figure 5-17. Photograph of Klamath and Shasta River Confluence at flood stage in December 31, 2005 and the average daily flow for that day was 11,100 cfs. Looking upstream and Shasta River is coming in from the right.

5.4. Bed Material

Multiple measurements of bed material were performed between 1999 and 2008 by PacifiCorp, Ayers, and Reclamation on the Klamath River and the data were included for this study. Additional pebble count samples were collected as part of this project in October of 2009 to verify the previous sampling. These samples will be referred to as Reclamation 2009.

PacifiCorp (2004b) performed pebble counts between Link Dam and Seiad Valley (RM 254 to 128). The representative diameters are shown in Figure 5-18 for the D16, D50, and D84, where D16 refers to the 16% of material having a diameter that is finer than the diameters found in the total sample. Some of the samples were collected to intentionally sample the finer material deposited during floods on higher bars not exposed to lower flows, in locations protected by large boulders, or in pools. They are not representative of the bed material that would control the bed elevations or of the bed armor layer.

Ayres (1999) performed a geomorphic assessment of the Klamath River below Iron Gate Dam and collected pebble counts from RM 5 to 130. Reclamation (2008) collected pebble count data to support a salmon redd scour study from RM 147 to 185. The representative particle diameters for all data collected downstream of Iron Gate Dam are given in Figure 5-19, Figure 5-20, and Figure 5-21 for the D16, D50, and D84, respectively.

The reach averaged D50 and computed stream power for Iron Gate Dam to Indian Creek is shown in Figure 5-22. There is a strong correlation between reach average stream power and the median diameter. As stream power increases, the river can move larger sediment particles; therefore, the surface sediment sizes left in the bed are larger. There are some exceptions to this correlation if there are changes to the sediment supply. Downstream of the Beaver Creek and Scott River the ratio of stream power to sediment diameter is larger indicating that the bed material is relatively more mobile at these locations. This would be consistent with the large coarse sediment load supplied by these tributaries, in particular the coarse sediment supply of Scott River.

These observations are consistent with Lane's sediment balance (Lane, 1955), which can be written as:

$$QS \propto Q_s d_{50} \qquad \text{Equation 5-1}$$

where Q is flow rate, S is slope, Q_s is sediment supply, and d_{50} is the median particle diameter of bed material load. As the flow rate or slope increases, the sediment supply or median particle diameter will increase.

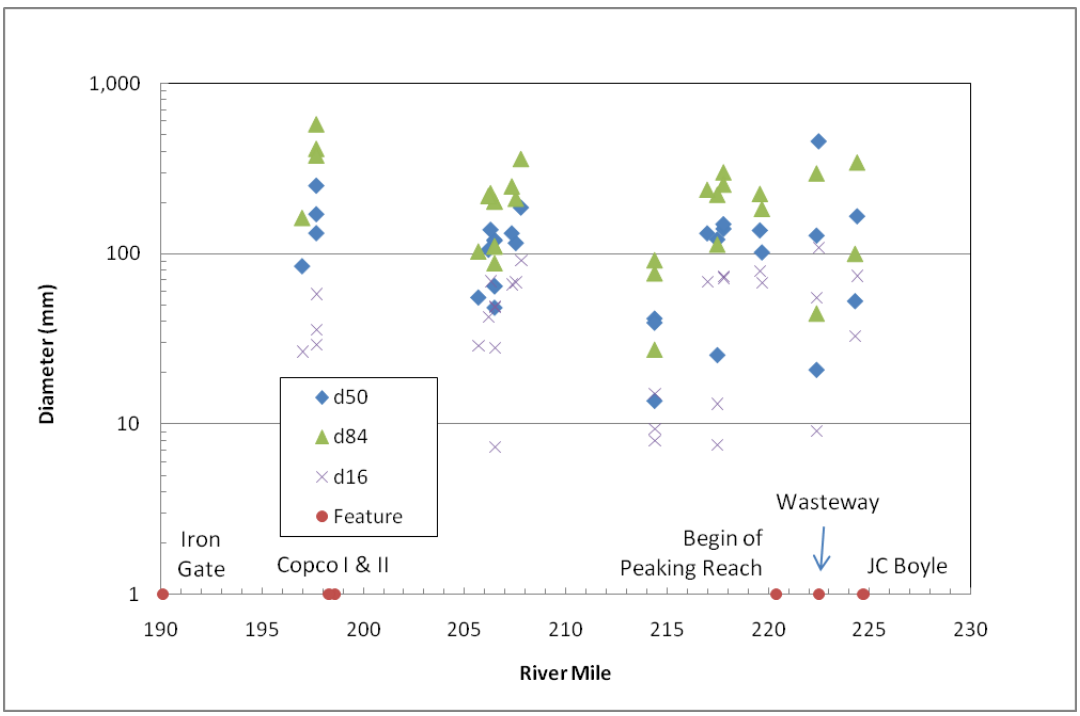

Figure 5-18. Measured representative bed material sizes in Klamath River downstream of J.C. Boyle and Upstream of Iron Gate reservoirs (PacifiCorp, 2004b).

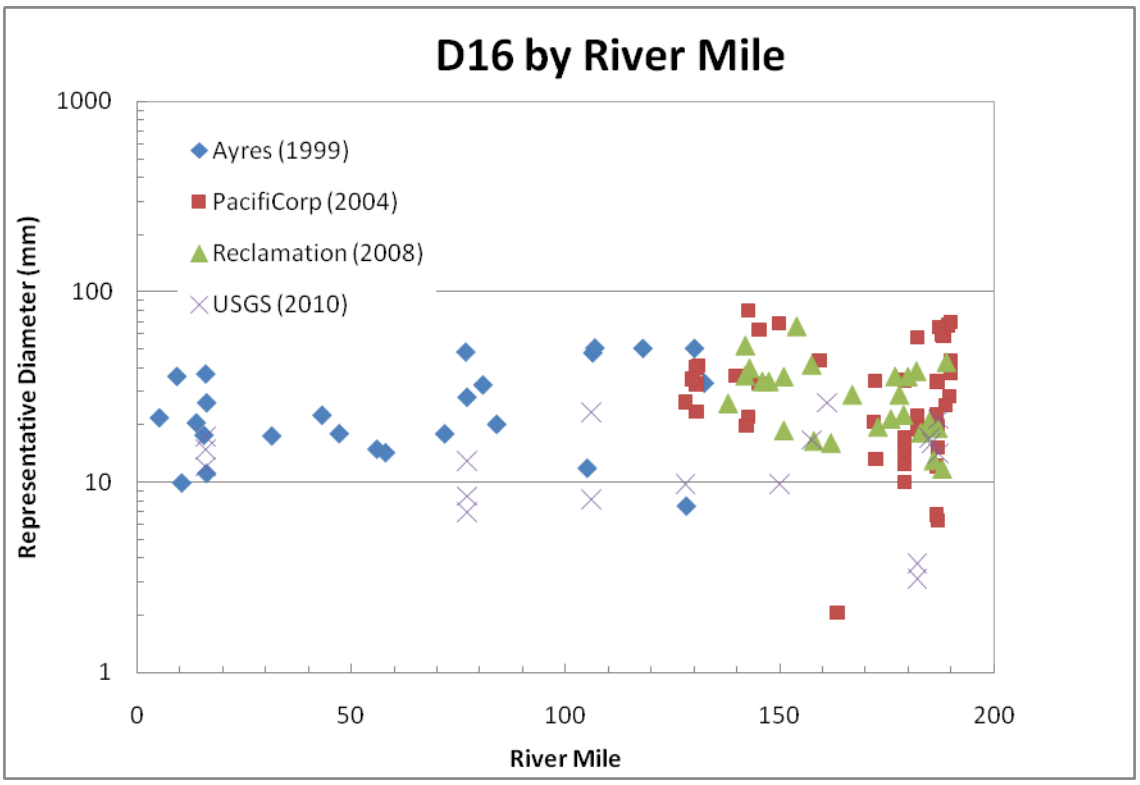

Figure 5-19. Measured D16 on Klamath River downstream of Iron Gate Reservoir.

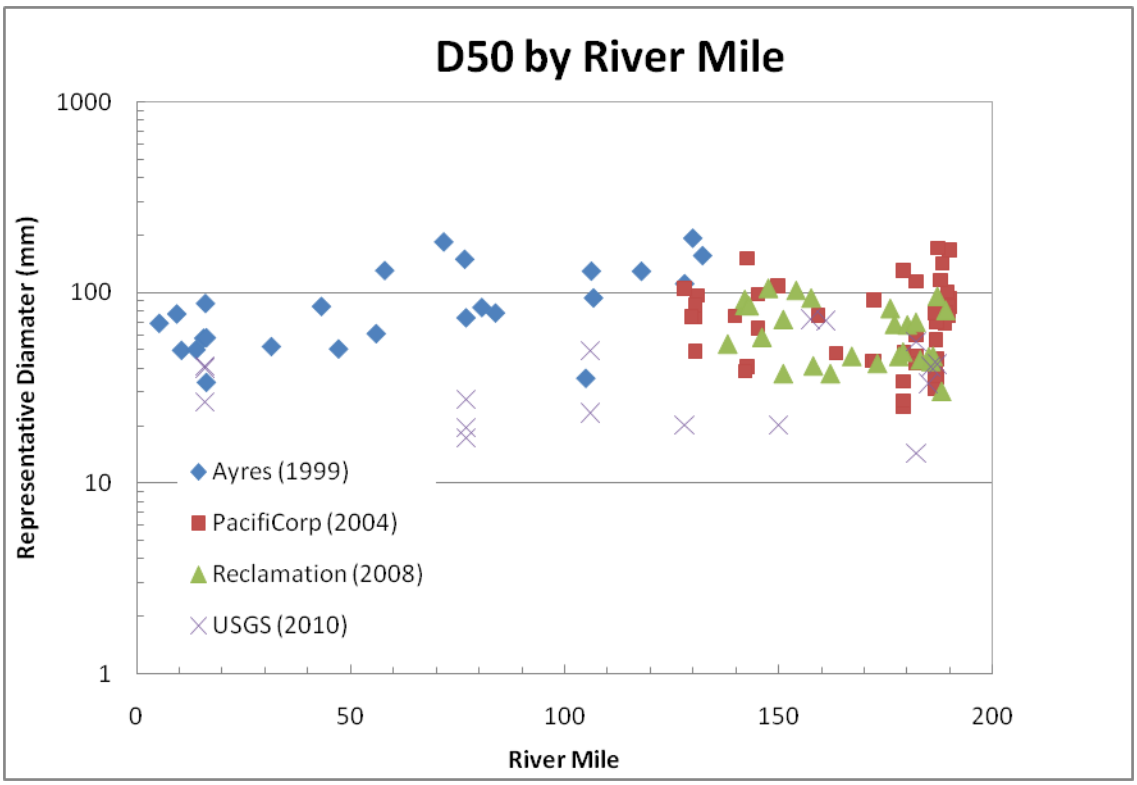

Figure 5-20. Measured D50 on Klamath River downstream of Iron Gate Reservoir.

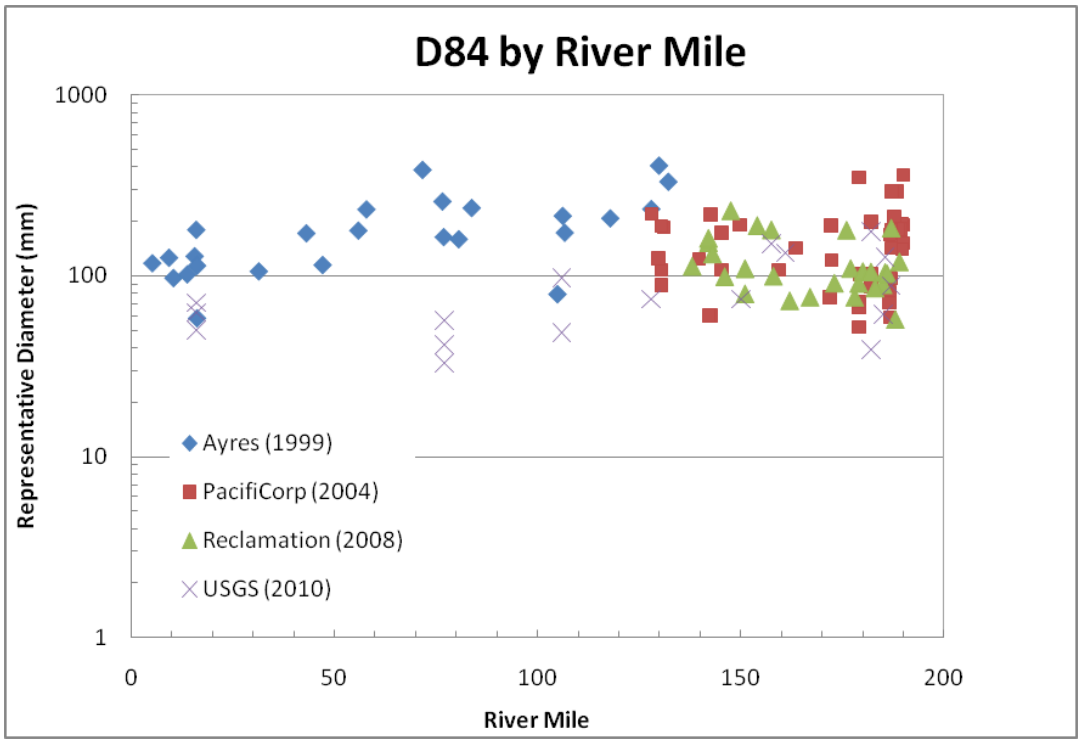

Figure 5-21. Measured D84 on Klamath River downstream of Iron Gate Reservoir.

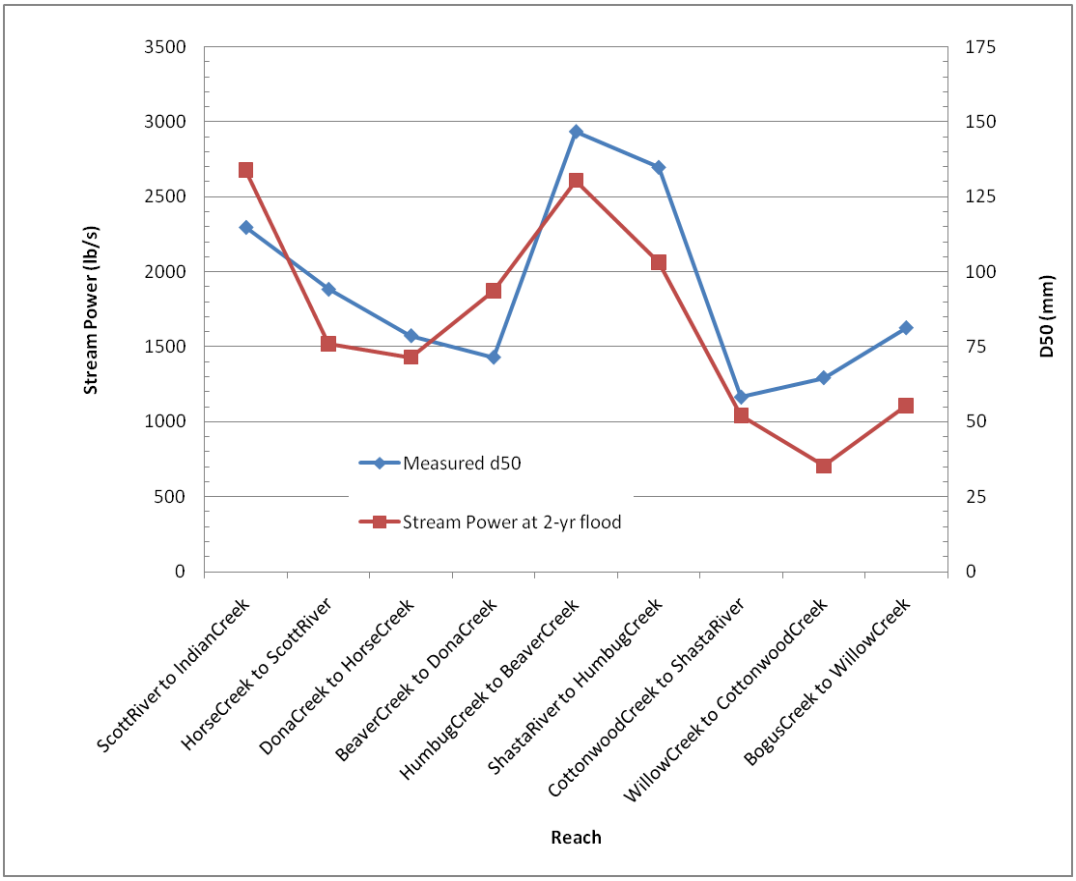

Figure 5-22. Average stream power and average D50 by reach.

5.5. Frequency of Mobilization

Several studies have estimated the magnitude of flow necessary to mobilize sediment in the Klamath River. All the studies used Shield's criterion is used to estimate gravel mobilization. The Shield's number, θ, is defined as:

$$\theta = \frac{\tau_g}{\gamma(s-1)D_{50}} \qquad \text{Equation 5-2}$$

where θ = dimensionless Shield's number; τ_g = grain shear stress; γ = specific weight of water; s = relative specific density of sediment; and D_{50} = median sediment size.

Often, there is a specific value above which bed motion is assumed to begin. However, sediment motion is more accurately described as a stochastic process and exact initiation of motion is a qualitative term. Parker (1990) suggests that the concept of initiation of motion be replaced by a reference amount of sediment motion described by a specific amount of non-dimensional sediment transport:

$$W^* = \frac{(s-1)gq_s}{\rho_s(\tau_g/\rho)^{1.5}} = 0.002 \qquad \text{Equation 5-3}$$

where s = relative specific density, g = acceleration of gravity, q_s = sediment transport rate, ρ_s = sediment density, τ_g = grain shear stress, ρ = water density. The Shields number that gives W^* = 0.002 is termed the reference Shield's stress (θ_r). It can be described as the condition when many particles are moving and there is a small, but measureable, sediment transport rate. The non-dimensional reference shear stress (θ_r) show considerable variation in the literature. A typical value for the reference Shield stress is about 0.02 to 0.04 (Parker, 1990; Buffington and Montgomery, 1998; Andrews, 2000; Wilcock and Crowe, 2003). However, there is significant variation and it has been found to vary between 0.01 and 0.1. Wilcock and Crowe (2003) use θ_r = 0.021 if the fraction of sand in the surface layer is above 0.2 and θ_r = 0.036 if the surface is devoid of sand. Lamb et al (2008) and Mueller et al. (2005) suggest that the critical or reference shear stress is dependent upon channel slope.

Appendix J. Reference Sediment Motion contains detailed information on the analytical methods used to compute Shields number at a variety of flows. Embedded in the method to compute the reference shear stress is the computation of the grain shear stress. The total shear stress is composed of the morphologic shear stress, the grain shear stress, and the wall shear stress (Lamb et al., 2008). The morphologic shear stress is that shear stress caused by bed forms and large channel features such as log jams or vegetation. A calculation of sediment mobilization should only include the grain shear stress.

If the shear stress is not increased beyond the reference shear stress, there will be only minimal disturbance of the armor layer. Many researchers suggest that a shear stress larger than the reference shear stress is necessary for significant disturbance of the armor layer. Hydraulic conductivity is a measure of the ability of water to travel through a permeable soil. Schälchi (1992) found that significant increases in hydraulic conductivity begin at $1.3\theta_r$. Higher hydraulic conductivities indicate a coarser bed that is flushed of fine material. Neill (1986) also suggests that significant mobilization occurs at $1.3\theta_r$. Holmquist-Johnson and Milhous (2010) also use the criteria proposing that the armor disturbance occurs at $1.3\theta_r$. The descriptions of slight mobilization, which is defined to occur at a $\theta = \theta_r$, and significant mobilization, which is defined to occur at $\theta = 1.3\theta_r$, is given in Table 5-5.

The exact definition of armor disturbance is somewhat artificial because the amount of transport will increase gradually and not as a step function, as shown in Figure 5-23 from Wilcock and Crowe (2003). Therefore, it is more accurate to analyze sediment transport as a continuum process rather than a process that has abrupt changes with flow rate. This implies the same amount of gravel movement would be accomplished by a high flow for a short duration as would be mobilized by a smaller flow for a longer duration. We suggest that the values definitions of slight mobilization and significant mobilization in Table 5-5 be used as general guidelines with the understanding that the mobilization of sediment is actually a gradual process, not marked by instantaneous jumps in transport with flow rate.

Table 5-5. Suggested general stages of sediment transport based upon Shield's number.

Relative Shield's Number	**Description**
θ_r	**Slight Mobilization**: There will be a small, but measurable, sediment transport rate. Armor layer is only minimally disturbed and there maybe flushing of sand to a depth of the D_{90}.
$1.3\ \theta_r$	**Significant Mobilization:** Many particles are moving and there is a significant sediment transport rate. Sand is mobilized in the interstitial spaces of the bed and to a depth of twice the D_{90}. The armor layer is significantly disturbed.

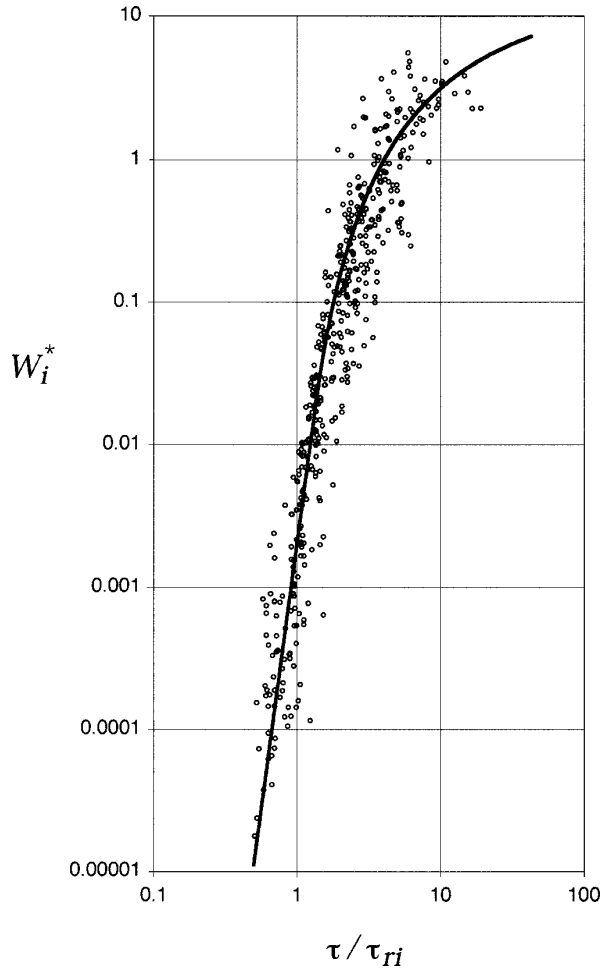

Figure 5-23. Figure 6 from Wilcock and Crowe (2003) showing relationship between non-dimensional transport rate (W_i*) and non-dimensional shear stress ($\theta/\theta_r = \tau/\tau_{ri}$) for a given size class *i*.

An issue related to the gravel mobilization is the mobilization of sandy material covering the bed or within the interstitial spaces of the gravel. The sandy material can move at much smaller shear stresses if it is exposed on the surface, but the sandy material located within the bed is protected by the larger gravels. Therefore, the depth of sand mobilization depends upon the mobilization of gravel. Wilcock et al. (1998) analyzed the sand mobilization on the Trinity River using measured data on sand transport and observations on sand coverage in the bed. Mobilization of sands within pools and the surface of the bed can occur at flows less than the flow required for mobilization of gravels. Wilcock et al. (1998) found that sands could be flushed to a depth of the D_{90} without gravel entrainment, but found that

fully mobilized gravel would flush sands to a depth of approximately twice the D_{90}. Diplas and Parker (1985) also found that fine sediment can be entrained to a depth of two to three times the surface layer thickness.

To predict the exact fraction of sand remaining in the bed after a flushing event, it is necessary to simulate the sand budget and bed mixing during the event. It is also necessary to obtain measurement of the surface and subsurface sand fractions as well as the sand supply in the reach. Wu and Chou (2003) and Cui (2006) have developed models to predict the flux of sand from the subsurface to the surface. Future studies of mobilization could be done to quantify the flows necessary to accomplish a certain level of sand mobilization in the Klamath River. These studies could improve our understanding of the amount of sand content in the bed previous to and after the high flow event.

There have been several previous studies of gravel mobilization in the Klamath River. Holmquist-Johnson and Milhous (2010) defined various levels of mobilization, from flushing of fines from interstitial spaces to armor disturbance. The critical value of Shield's parameter for armor disturbance was 0.045, and based upon their descriptions of motion, reference sediment motion is assumed to occur at 0.035. They also assumed that the morphologic and wall shear stress was zero. The main purpose of removing fine sediment in the Klamath River is to increase salmon habitat and decrease the occurrence of *C. shasta*, which is a bacteria that infects salmon. However, it is uncertain exactly how much habitat is destroyed from a specific mobilization flow and how much mobilization of fine material is necessary to control *C. shasta*.

Ayres (1999) measured bed material and cross sections at six locations on the Klamath River from Iron Gate Dam to the Pacific Ocean. They assumed that θ_r = 0.035. They assumed that the morphologic and wall shear stress was zero.

PacifiCorp (2004b) analyzed sediment motion at several other locations along the river as well. They used measured cross section data and bed material data to estimate mobilization under the No Action Alternative. They also computed mobilization flows under the Dam Removal Alternative by assuming a bed material size based upon tributary bed material sizes upstream of Iron Gate Dam. They also assumed that this bed material size would be the same for the entire length of the Klamath River below Iron Gate. PacifiCorp used θ_r = 0.047 and assumed that the morphologic and wall shear stress was zero.

Table 5-6. Previous estimates of the flow required to for Slight Mobilization ($\theta = \theta_r$) on the Klamath River.

		No Action			**Dam Removal**
Location (RM)	**Description**	**Ayres (1999)**	**PacifiCorp (2004b)**	**USGS (2010)**	**PacifiCorp (2004b)**
16.3	Below Blue Creek Confluence	147,000	-	-	-

77	Sandy Bar	59,000	-	-	-
106	Happy Camp	33,500	-	-	-
128	Portuguese Creek	16,500	68,000	-	27,000
161	Beaver Creek	13,000	-	-	-
172	Tree of Heaven	-	17,329	-	8,700
187	Little Bogus Creek	9,800	9,700	8,700	6,600

5.5.1. CURRENT ESTIMATES OF MOBILIZATION

Using the average hydraulic properties and averaged D50 of each reach, it is possible to estimate the reach averaged slight mobilization flow and the reach averaged significant mobilization flow. The return period of the initiation of flow is also calculated. The methods used to compute sediment mobilization are described in

Appendix J. Reference Sediment Motion. Mobilization is assumed to occur when the shear stress applied to the sediment particles of the bed exceeds the reference shear stress. There is considerable uncertainty in defining the mobilization flow without direct field measurements of sediment movement. One major uncertainty is the value of the reference shear stress. Based upon the previous studies, a range of 0.025 to 0.035 in shear stress is estimated for reference sediment motion to represent the probable range of potential mobilization on the Klamath River. Only the grain shear stress is used to compute shear stress applied to sediment mobilization. Previous studies have used the total shear stress and have not accounted for the inherent uncertainty in this estimate without measurements of sediment bedload movement.

Figure 5-24 shows the flow at which mobilization will occur on a reach average basis for the reaches defined in Section 4.2. The reach from Iron Gate Dam to Bogus Creek is not shown because there are no direct measurements of bed material size in this reach. It is expected that this reach is essentially fully armored because there has been no significant sediment supply to this reach for almost 50 years.

The median estimate of the slight mobilization flow from Bogus Creek to Willow Creek is about 9,500 cfs. This is consistent with the Ayres (2009) and USGS (2010) who found the mobilization flow to be 9,800 cfs and 8,700 cfs, respectively. The potential range of the mobilization flow in this reach is expected to be from 7,000 to 13,000 cfs. Field measurements of sediment mobilization are needed to reduce the uncertainty of this value. The range of the return period of the mobilization flow is between 2.6 to 7.5 years in the Bogus Creek to Willow Creek reach.

The reach between Cottonwood Creek and the Shasta River has a slightly smaller mobilization flow than the reaches upstream, corresponding to the supply of material from Cottonwood Creek. The return period of the mobilization flow is significantly less than the reaches between Iron Gate and Cottonwood Creek.

The mobilization flow increases substantially downstream of Shasta River to Beaver Creek. This reach is steeper than the reaches upstream or downstream of it. The bed elevations in this reach are primarily controlled by relatively immobile large cobbles, boulders, and bedrock. The sediment quickly moves through the reach, and therefore it is essentially a “pass through” reach.

At Beaver Creek, the tributary supply of peak flows and additional sediment in this reach decrease the mobilization flow substantially. The return period of slight mobilization is between 1.25 and 1.5 years. (A return period of 1.5 years is typical of gravel-bed rivers with unimpaired hydrology and sediment regimes).

At Scott River, the mobilization flow increases substantially, but the median return period for slight mobilization is still less than 2 years. Scott River supplies

large amounts of sediment and also substantially increases the peak flow of the Klamath River.

Table 5-7. Low, median, and high estimates of bed material initiation of mobilization flow under current conditions ($\theta = \theta_r$).

Reach	Slight Bed Material Mobilization Flow Estimates (cfs)		
	Low	**Median**	**High**
Bogus Creek to Willow Creek	7,000	9,800	13,100
Willow Creek to Cottonwood Creek	7,700	10,700	14,200
Cottonwood Creek to Shasta River	5,900	8,400	11,300
Shasta River to Humbug Creek	14,000	20,000	27,400
Humbug Creek to Beaver Creek	13,500	19,100	26,400
Beaver Creek to Dona Creek	3,900	5,800	8,000
Dona Creek to Horse Creek	4,200	5,900	7,900
Horse Creek to Scott River	4,700	6,500	8,600
Scott River to Indian Creek	11,000	15,300	20,500

Table 5-8. Low, median, and high estimates of significant bed material mobilization flows under current conditions ($\theta = 1.3\theta_r$).

Reach	Significant Bed Material Mobilization Flow Estimates (cfs)		
	Low	**Median**	**High**
Bogus Creek to Willow Creek	11,500	15,900	21,300
Willow Creek to Cottonwood Creek	12,500	17,200	22,900
Cottonwood Creek to Shasta River	9,700	13,800	18,400
Shasta River to Humbug Creek	23,800	33,900	45,800
Humbug Creek to Beaver Creek	22,600	32,900	45,500
Beaver Creek to Dona Creek	6,900	10,100	13,900
Dona Creek to Horse Creek	6,900	9,700	13,200
Horse Creek to Scott River	7,500	10,400	13,900
Scott River to Indian Creek	17,900	25,500	34,100

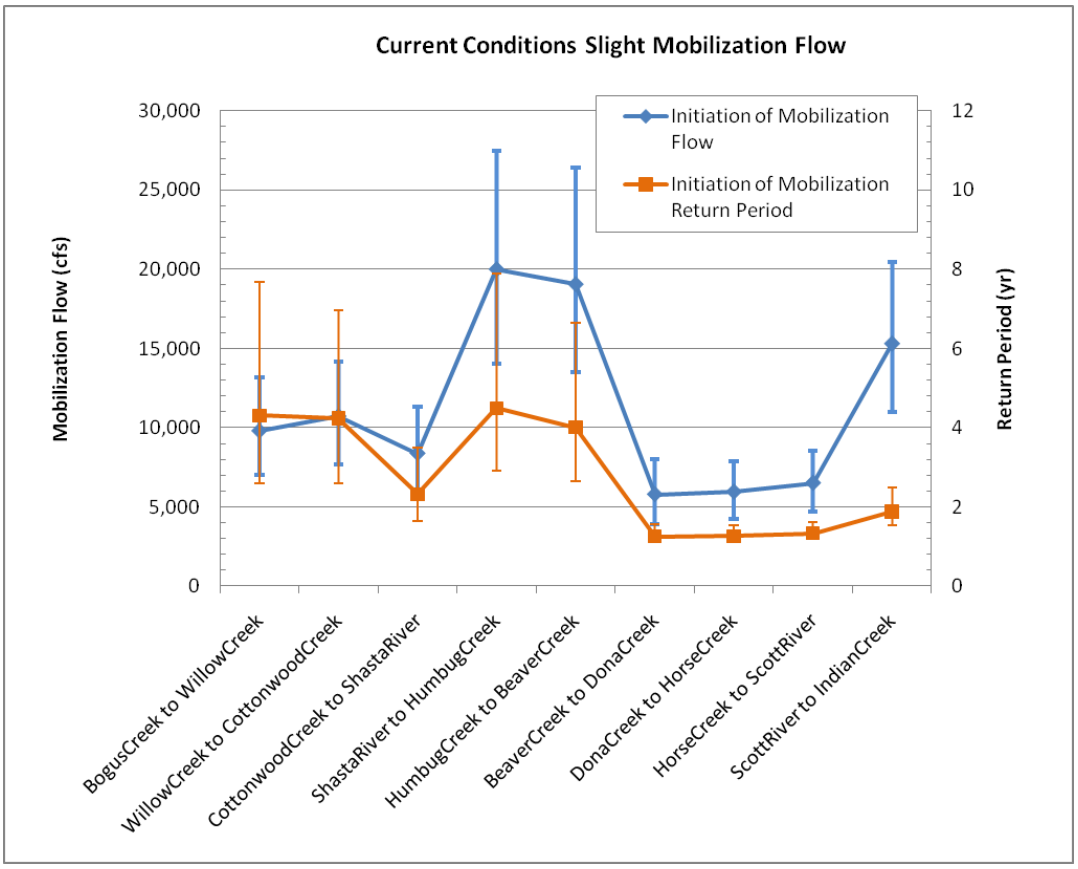

Figure 5-24. Slight bed material mobilization flow and return period for reaches downstream of Iron Gate Dam.

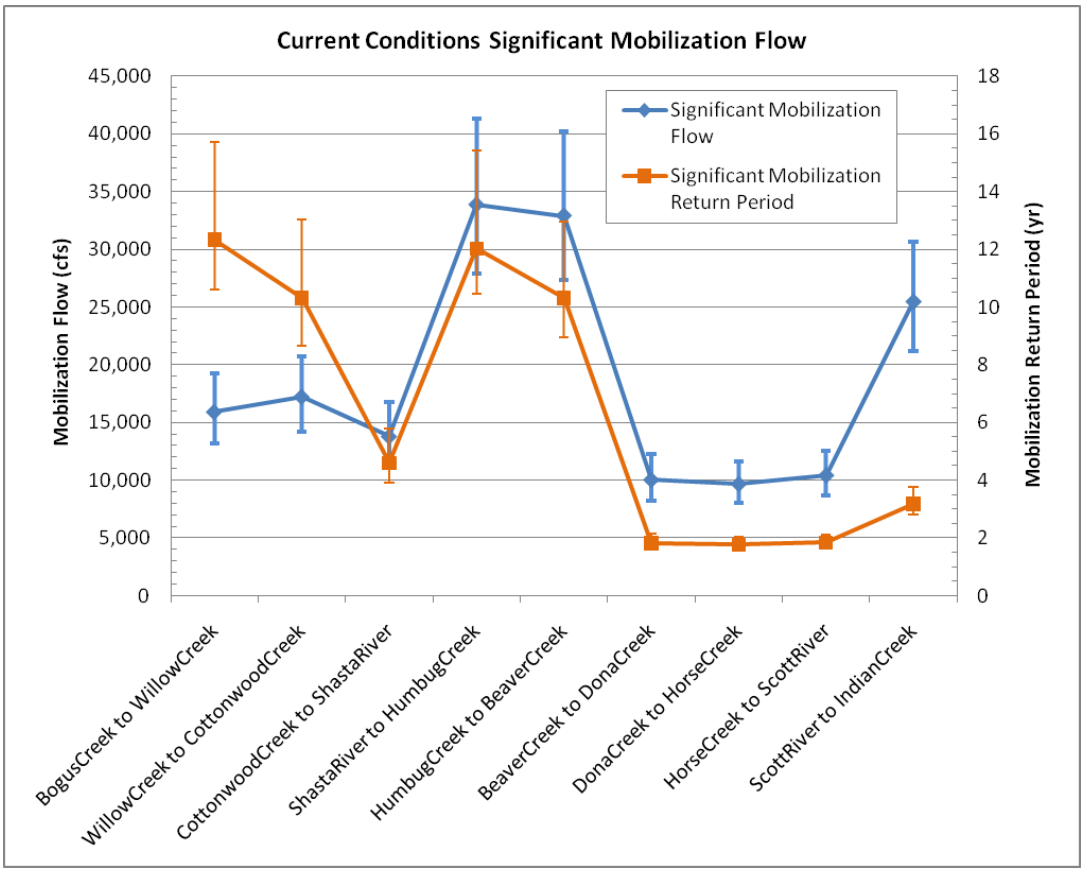

Figure 5-25. Significant bed material mobilization flow and return period on a reach averaged basis for reaches downstream of Iron Gate Dam.

5.6. Reservoir Sediment

A detailed reservoir investigation is documented in Reclamation (2010) and relevant results are reproduced here. Previous reservoir investigations have been performed by J.C. Headwaters, Inc. (2003), and Shannon and Wilson (2006).

Sediment in the reservoirs was characterized by soil properties, grain size, desiccation properties, and critical shear stress. The soil properties, including grain size and critical shear stress, were determined from field sampling and laboratory testing.

Field investigations were conducted at J.C. Boyle, Copco No. l, Copco No. 2, and Iron Gate dams/reservoirs, and in the Klamath River Estuary including about seven miles upstream from the mouth of the river. Maps of the reservoir and the sample site locations are given at the end of this section in Figure 5-26, Figure 5-27, and Figure 5-28, for J.C. Boyle, Copco 1, Iron Gate dams/reservoirs, and the Klamath River Estuary, respectively. Phase 1 of the geologic investigations included in-reservoir drilling to collect comprehensive suites of samples of reservoir sediment (Qr) behind each dam. There were three main purposes of this work:

1. To collect samples for screening-level analysis of organic and inorganic chemical compounds within the reservoir sediment and, where present, to determine the level and extent of contamination.

2. To collect samples of reservoir sediment to determine a standard suite of physical properties and to collect undisturbed samples for analyses of engineering properties.

3. To help determine the thickness of reservoir sediment throughout all major sections of each reservoir.

The in-reservoir geologic investigations consisted of:

- Barge and boat platforms for Auger Drilling and Sampling
- Barge and boat platforms for Push Tube Sampling
- A boat platform for Vibracore Drilling and Sampling
- A boat platform for Gravity Tube Sampling

Barge and boat-supported drilling/sampling took place at fifty-five locations in J.C. Boyle, Copco No.1, and Iron Gate reservoirs. Sixty-nine samples of reservoir sediment and pre-reservoir deposits were collected for gradation analysis, Atterberg limits, and field moisture content; seventy-three samples of reservoir sediment were collected for chemical analysis; and nineteen undisturbed samples of reservoir sediment were collected in Lexan liners for engineering properties,

such as shear strength, testing. In Copco No. 2 Reservoir, boat-supported sampling of reservoir sediment was performed at sixteen locations, from the dam upstream for about 1,000 feet. In the Klamath River Estuary and up to seven miles upstream, boat-supported sampling took place at five locations, and characterization of fluvial deposits was conducted along seven miles of the river banks.

Fine-grained sediment in all of the reservoirs consisted primarily of Elastic Silt (MH), with lesser amounts of Elastic Silt with Fine Sand. The reservoir sediment is mostly an accumulation of silt-size particles of organic material, such as algae and diatoms, and silt-size particles of rock loosely arranged in an open water-filled structure. Reservoir sediment hosts a higher percentage of silt, sand, and gravel in the upper reaches of each reservoir. From the upper reaches to several thousand feet downstream, this coarse sediment transitions into deposits of sandy elastic silt, and then into elastic silt with trace sand.

Fine-grained reservoir sediment (Elastic Silt) throughout all the reservoirs has the consistency of pudding. The sediment captured in the sample tubes was very soft and indented with very light finger pressure. At 6 to 10 feet in the sample tubes, the sediment firmed up a little. On a microscopic scale, it has an open structure that holds a very high water content. Field moisture of samples of Elastic Silt were frequently 200% to 300% of the sample's dry weight, and ranged up to 700% moisture. Most reservoir sediment having this high water content that remains after the initial stage of dam removal will take some time to dry out.

Fine-grained reservoir sediment has a low cohesion and is highly erosive. In each reservoir, fine-grained reservoir sediment was thinnest in the upstream portion of the reservoir and thickest near the dam. Reservoir sediment was also thin to nonexistent in narrow channels of the reservoirs where water flow was greater than an estimated 2 to 4 miles per hour. This was attributed to the sediment either remaining in suspension or eroding from the active channel, or both.

These investigations demonstrated that sediment deposition throughout all four reservoirs follows well-understood principals of geology and of fluvio-lacustrine sedimentation. Geologic investigations did not encounter any unusual characteristics of the sediment or unique depositional environments requiring special consideration or explanations.

Methane gas is currently trapped in reservoir sediment behind each dam and this gas will escape during reservoir drawdown. A screening-level determination for all potential contaminants within the reservoir sediments is to be made by Reclamation in separate reports.

Surface geologic mapping and the installation of groundwater observation wells around each reservoir are planned for Phase 2 of the investigation program.

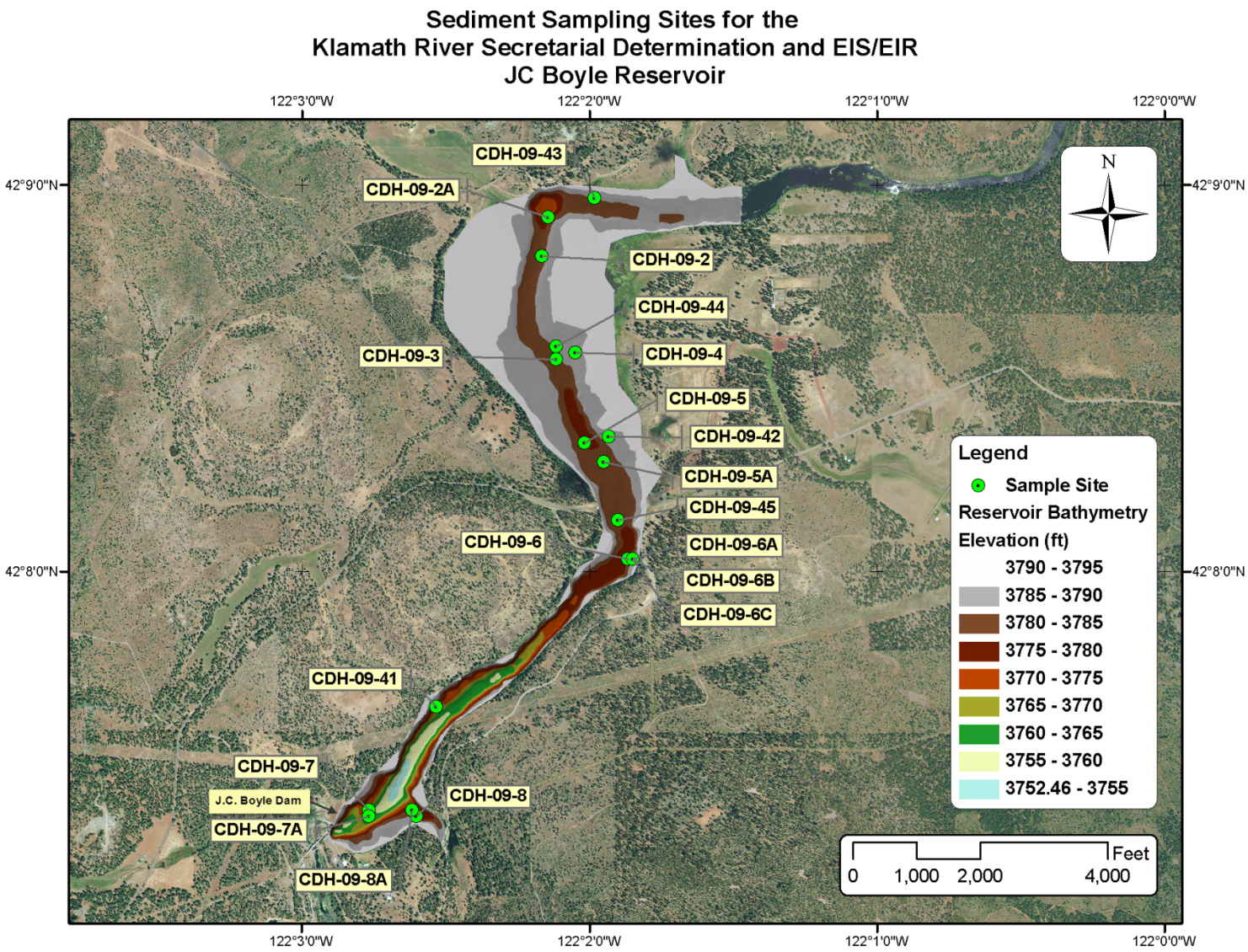

Figure 5-26. Bathymetry of J.C. Boyle Reservoir and 2009 drill hole locations.

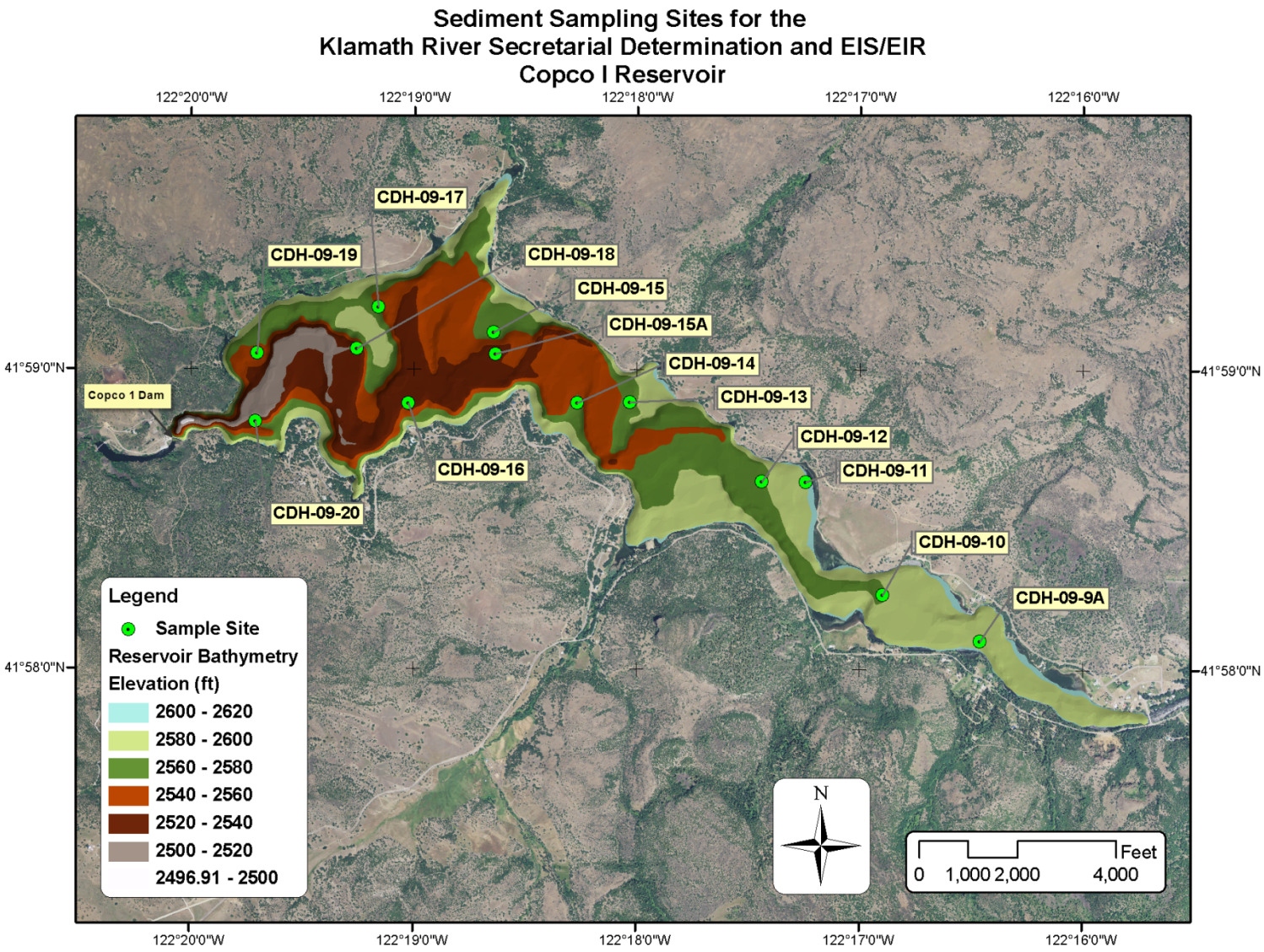

Figure 5-27. Bathymetry of Copco Reservoir and 2009 drill hole locations.

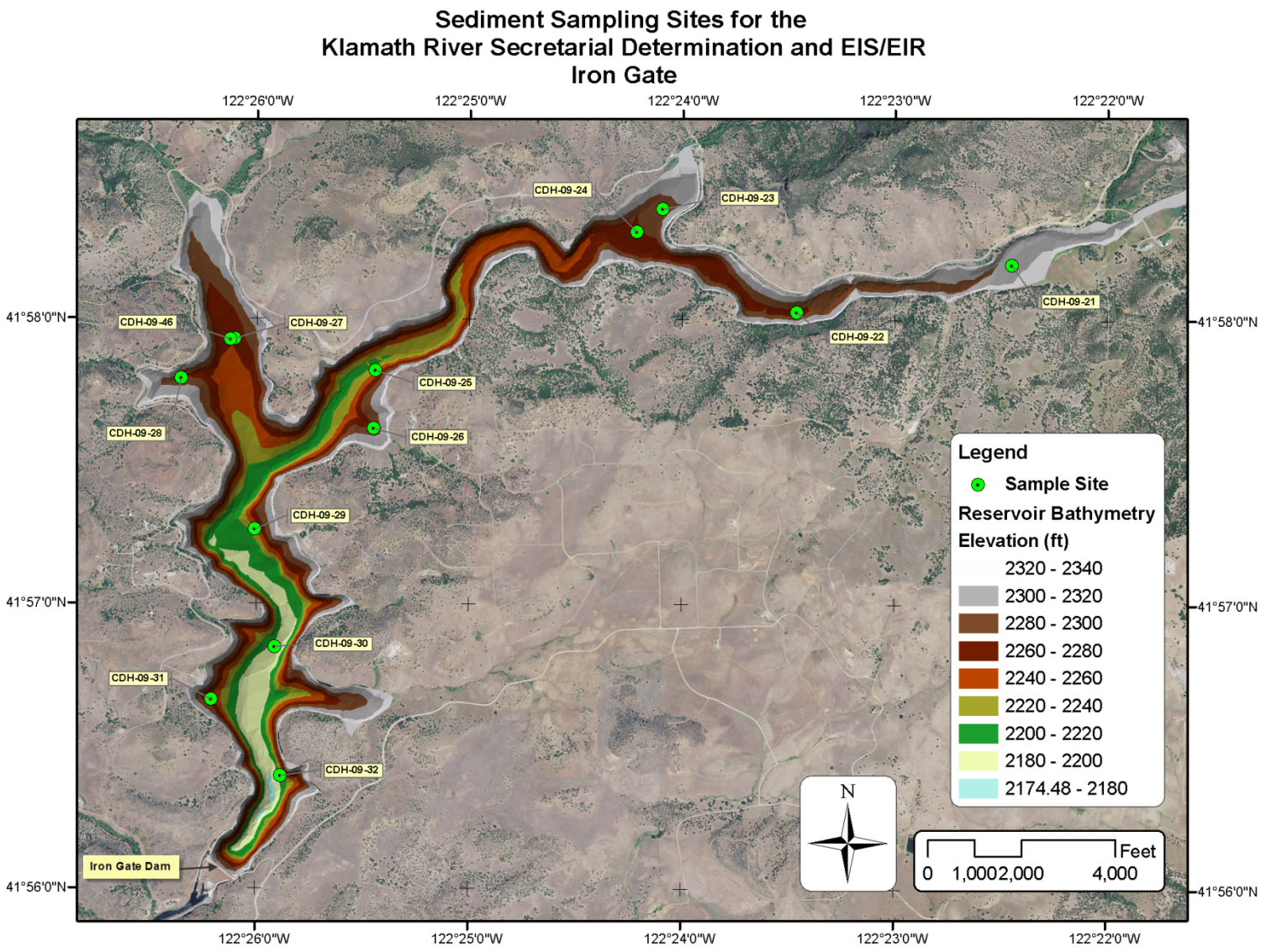

Figure 5-28. Bathymetry of Iron Gate Reservoir and 2009 drill hole locations.

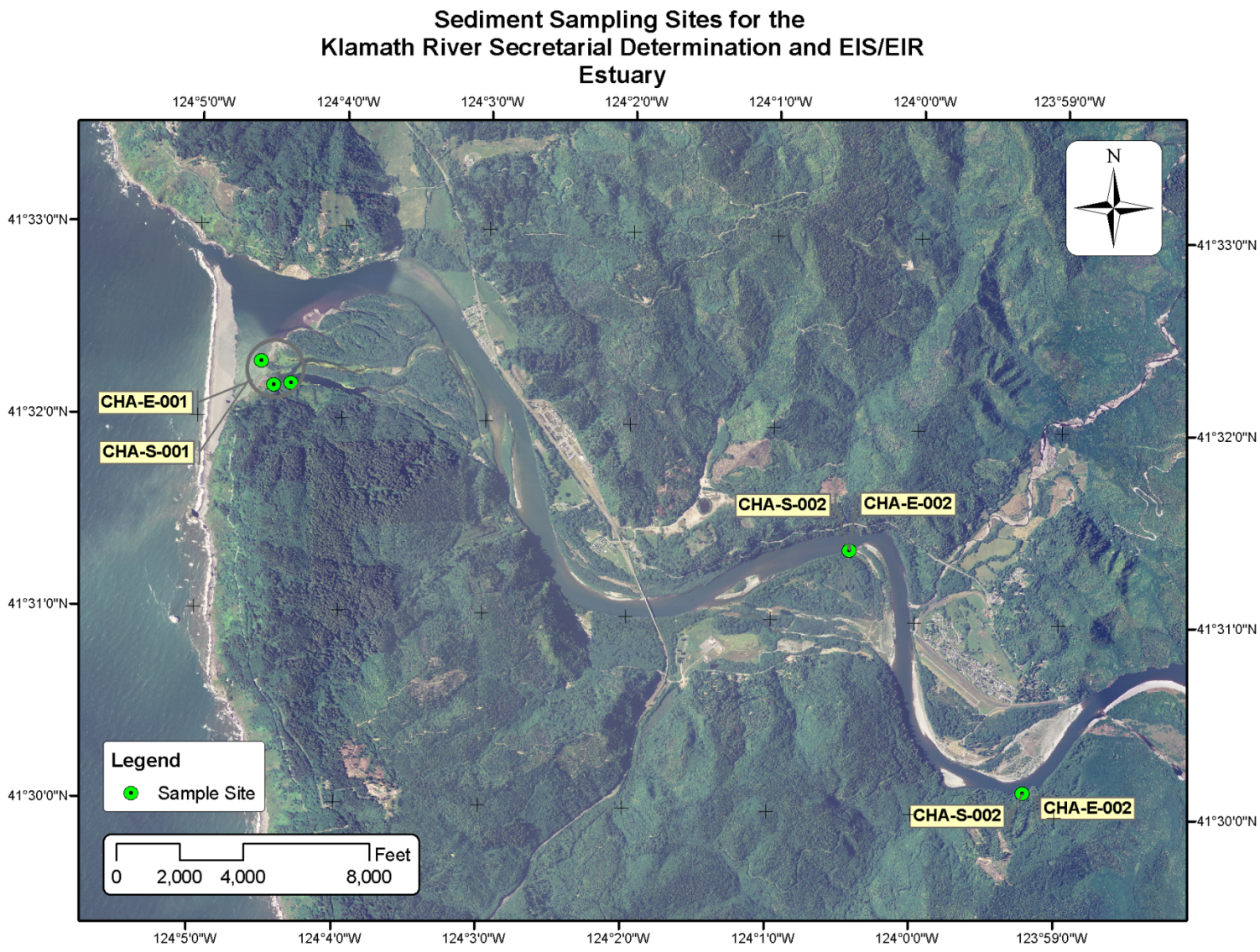

Figure 5-29. 2009 Sample site locations in the Klamath River Estuary.

5.6.1. SEDIMENT VOLUME AND THICKNESS

This section will detail the previous estimates of reservoir sediment volumes and explain the methodology for obtaining new volume estimates.

5.6.1.1. Previous Estimates

There have been two different estimates of the reservoir volumes. JC Headwaters, Inc. (2002) performed a bathymetric survey of J.C. Boyle, Copco No. 1, and Iron Gate reservoirs. JC Headwaters, Inc. (2002) then computed the relationships between reservoir storage volume and reservoir elevation. These were compared against the historical relationships based upon the pre-dam survey of each reservoir. The difference at full pool between the historical storage volume and the current storage volume was assumed to be the volume of sediment deposition. GEC (2006) estimated the reservoir volume based a difference between upon pre-dam surveys and the survey of JC Headwaters, Inc. (2002). The results of the two methods are given in Table 5-9.

Shannon and Wilson (2006a) collected sediment samples to characterize the physical and chemical properties of the sediment trapped behind the reservoirs. The reservoir sediment depth was recorded at 26 sites in J.C. Boyle, Copco 1, and Iron Gate reservoirs.

Table 5-9. Previous reservoir sediment volume estimates.

	Reservoir sediment (yd^3)			
Study	**J.C. Boyle**	**Copco No. 1**	**Copco No. 2**	**Iron Gate**
GEC (2006)	636,000	10,870,000	None	8,767,000
JC Headwaters, Inc. (2003)	22,222	9,629,000	None	4,818,000

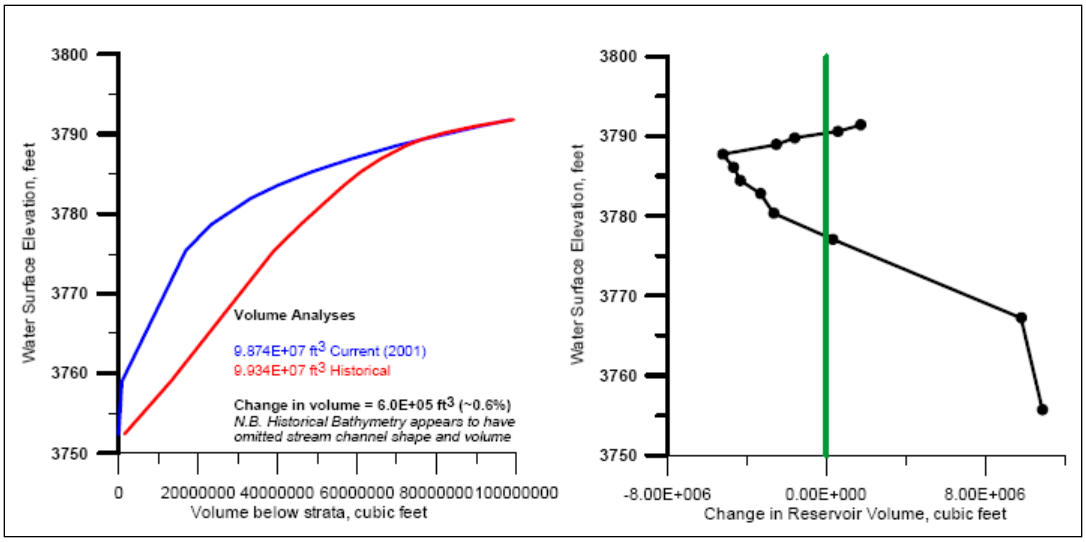

Figure 5-30. Volume – Elevation data for J.C. Boyle Reservoir. From J.C. Headwaters, Inc. (2003).

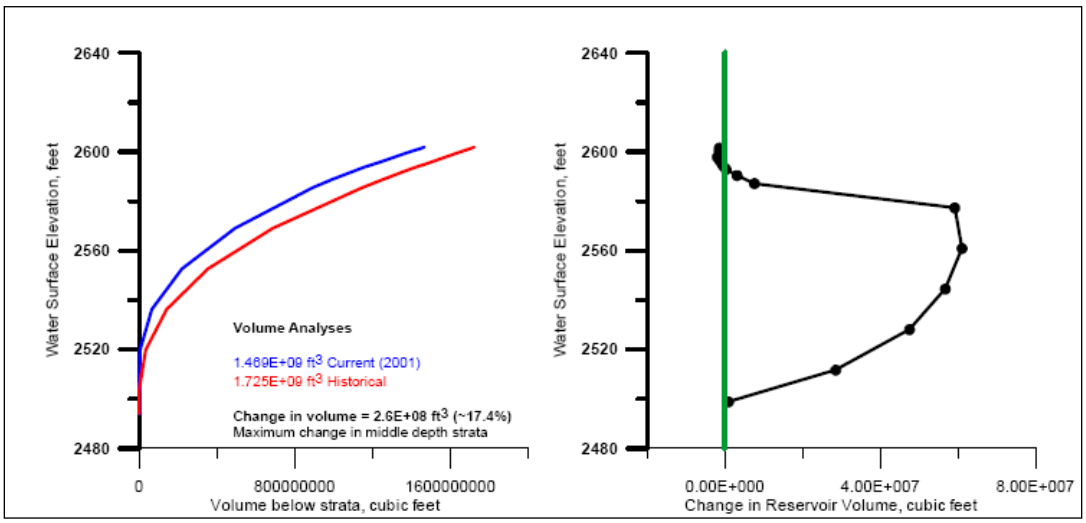

Figure 5-31. Volume – Elevation data for Copco No. 1 Reservoir. From J.C. Headwaters, Inc. (2003).

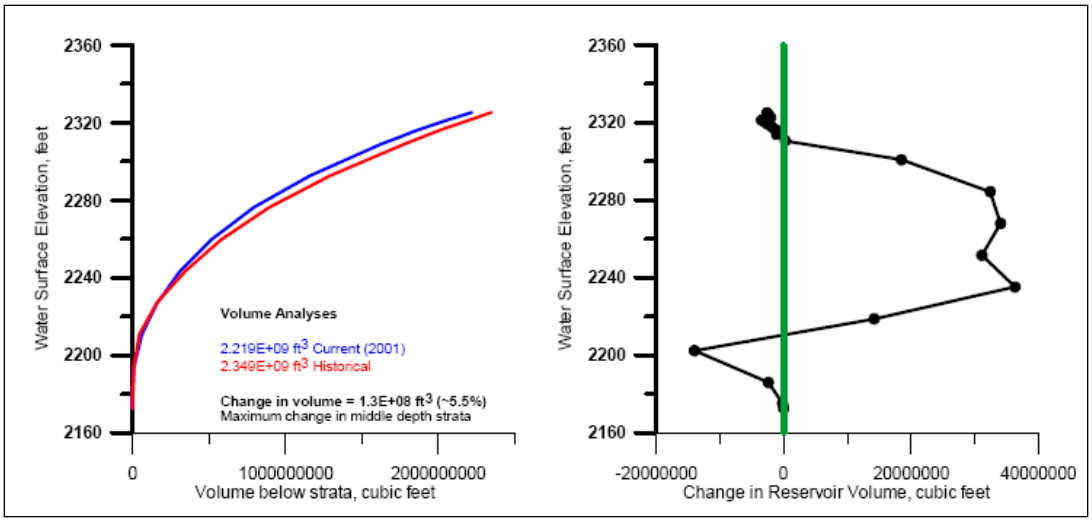

Figure 5-32. Volume – Elevation data for Iron Gate Reservoir. From J.C. Headwaters, Inc. (2003).

5.6.1.2. Current Estimates

A limitation of previous volume estimates is that they relied upon the pre-dam surveys. At Copco 1 Dam, the pre-dam contour interval was 5 feet. At Iron Gate and J.C. Boyle dams, the contour interval was 10 feet. The reservoir sediment thicknesses were generally less than 10 feet at Copco Reservoir, less than 5 feet at Iron Gate Reservoir and less than 20 feet at J.C. Boyle Reservoir. The sediment thicknesses were generally equivalent to the contour interval, making it difficult to obtain accurate estimates of the thickness through differencing of surveys. A much more direct way to estimate the sediment volumes is to rely upon the upon the drill holes, which are direct measurements of the sediment thickness. To develop sediment thickness measurements for the entire reservoir, measurements were extrapolated from the work of Shannon and Wilson (2006) and from Reclamation (2010).

JC Boyle

The sediment depth at J.C. Boyle Reservoir was determined by combining the sediment sample information with field observations. In the upper portions of the reservoir, little or no sediment was found during drilling except in one bend of the historical stream channel. An estimate of the extent and approximate location of this sediment deposition was drawn on the map to encompass the drill holes where the sediment was sampled. The extent of the deposition was limited to the historical stream channel.

In the lower portion of the reservoir, the sediment samples were used to determine the thickness. Holes CDH-09-07 (near the dam) and CDH-09-6 (near the state highway bridge) were near the dam and the sediment thickness was linearly interpolated between them. Table 5-10 shows the sediment samples used.

Figure 5-35, at the end of this section, shows the map of reservoir thickness and the locations of the Shannon and Wilson (2006a) and 2009 sediment samples. The volume of trapped sediment was estimated to be 990,000 yd^3. Limited samples available where the sediment was the deepest near the dam contributed to the considerable uncertainty in this estimate. It is expected that the uncertainty of the estimate is about +/- 30% or 300,000 yd^3. The previous GEC estimate was 600,000 yd^3 and it is likely that the true value is somewhere in between this estimate and the current one. Additional drill holes in the areas where significant sediment is present could reduce this uncertainty. Specifically, more samples could be taken in the 4,000 feet nearest the dam.

Table 5-10.Sediment sample locations and depths for J.C. Boyle Reservoir.

Year	Sample Number	Latitude	Longitude	Sediment Depth (ft)	Station (ft)	Bed Elevation (ft)
2006	J-1	N42 7.34	W122 2.782	13.2	191010.8	3766
2006	J-2	N42 8.921	W122 1.781	0	204732.9	3783
2006	J-3	N42 7.998	W122 1.968	0.5	196573.9	3776
2006	J-4	N42 8.926	W122 2.148	0.3	203054	3770
2006	J-5	N42 8.625	W122 2.197	0.3	201158.7	3779
2009	CDH-09-2	N42 08 49.6	W 122 02 10.8	5	202437.3	3779.02
2009	CDH-09-3	N42 08 33.7	W 122 02 07.5	6	200666.4	3781.4
2009	CDH-09-4	N42 08 34.2	W 122 02 03.3	9	200531	3785.7
2009	CDH-09-4A	N42 08 34.2	W 122 02 03.3	9.2	200531	3785.7
2009	CDH-09-5	N42 08 20.6	W 122 02 01.6	0.3	199182	3777.3
2009	CDH-09-5A	N42 08 02.1	W 122 01 51.8	0.3	197032.2	3777.3
2009	CDH-09-6	N42 08 02.5	W 122 01 52.6	0	197060.9	3777.6
2009	CDH-09-6A	N42 08 01.8	W 122 01 51.6	0	197030.4	3777.5
2009	CDH-09-6B	N42 08 02.1	W 122 01 51.8	0	197032.2	3777.5
2009	CDH-09-6C	N42 08 02.2	W 122 01 51.4	0	197047.8	3777.6
2009	CDH-09-7	N42 07 23.0	W 122 02 46.0	18.7	191256.4	3762.6
2009	CDH-09-7A	N42 07 22.9	W 122 02 46.0	21.7	191249	3762
2009	CDH-09-8	N42 07 22.4	W 122 02 36.8	1.7	191607.9	3779.8
2009	EDH-09-1	N42 08 49.5	W 122 02 11.0	3.2	202424.5	3779.1
2009	EDH-09-1A	N42 08 49.0	W 122 02 10.4	3.4	202384.3	3779.1
2009	EDH-09-2	N42 08 35.0	W 122 02 08.5	9	200797.6	3785.63
2009	EDH-09-2A	N42 08 34.1	W 122 02 09.3	9	200804.3	3785.8
2009	EDH-09-3	N42 07 26.2	W 122 02 41.0	14	191766	3756.3

Copco 1

To estimate the sediment depth throughout Copco 1 and Iron Gate reservoirs, a relationship was found between sediment depth and position within the reservoir for collected sediment samples. Samples were measured by Shannon and Wilson (2006a) and Reclamation (2009). For Copco Reservoir, 28 samples were used. Table 5-11 shows the samples used.

Table 5-11 Sediment sample locations and depths for Copco 1 Reservoir.

Year	Sample Number	Latitude	Longitude	Sediment Depth (ft)	Station (ft)	Bed Elevation (ft)	Relative Station	Relative Bed Elevation	Predicted Sediment Depth (ft)
2006	C-02	N41 58.154	W122 16.828	4.4	67610.69	2586.91	0.75	0.44	4.0
2006	C-03	N41 58.585	W122 17.88	5.7	61763.27	2575.96	0.50	0.45	4.3
2006	C-04	N41 58.829	W122 18.147	7.7	59876.47	2553.73	0.42	0.72	7.0
2006	C-05	N41 59.358	W122 18.781	5.8	56491.14	2555.35	0.27	0.58	5.8
2006	C-06	N41 58.921	W122 18.992	10	55386.44	2527.04	0.23	0.88	8.8
2006	C-07	N41 57.93	W122 16.244	5.8	70858.52	2590.68	0.89	0.54	4.8
2006	C-08	N41 58.373	W122 17.246	3.6	65168.13	2579.21	0.65	0.51	4.8
2006	C-09	N41 59.123	W122 18.277	3.5	58374.78	2561.33	0.36	0.56	5.5
2006	C-10	N41 58.908	W122 19.367	9.4	53632.49	2521.01	0.15	0.88	8.8
2006	C-12	N41 57.874	W122 16.04	6	71828.75	2588.39	0.93	0.77	6.8
2009	CDH-09-09A	N41 58.096	W 122 16.460	4.6	69356.10	2588.15	0.83	0.55	4.9
2009	CDH-09-10	N41 58.251	W 122 16.896	8	67052.88	2577.04	0.73	0.68	6.2
2009	CDH-09-11	N41 58.627	W 122 17.241	1.3	63999.20	2598.66	0.60	0.15	1.4
2009	CDH-09-12	N41 58.629	W 122 17.4403	5.4	63397.06	2573.55	0.57	0.58	5.5
2009	CDH-09-13	N41 58.892	W 122 18.031	5.7	60065.93	2566.99	0.43	0.55	5.3
2009	CDH-09-14	N41 58.889	W 122 18.268	5.3	59234.95	2562.94	0.39	0.34	3.3
2009	CDH-09-15	N41 59.124	W 122 18.642	3	57029.61	2569.58	0.30	0.50	4.9
2009	CDH-09-15A	N41 59.052	W 122 18.634	9.7	57070.02	2536.23	0.30	0.87	8.6
2009	CDH-09-16	N41 58.888	W 122 19.025	7.5	55224.26	2531.46	0.22	0.85	8.5
2009	CDH-09-17	N41 59.208	W 122 19.160	1.2	54706.02	2555.67	0.20	0.28	2.8
2009	CDH-09-18	N41 59.0680	W 122 19.256	9.2	54196.37	2523.17	0.18	0.92	9.2
2009	CDH-09-19	N41 59.053	W 122 19.704	4.8	51685.14	2552.44	0.07	0.50	5.1
2009	CDH-09-20	N41 58.825	W 122 19.711	7.4	51509.81	2534.69	0.06	0.78	8.0
2009	EDH-09-04	N41 58 12.2	W 122 16 42.1	3.5	67988.99	2590.08	0.77	0.57	5.2
2009	EDH-09-05	N41 58 53.4	W 122 17 51.8	1.9	60597.71	2579.53	0.45	0.31	3.0
2009	EDH-09-05A	N41 58 53.4	W 122 17 51.9	1.8	60597.71	2579.53	0.45	0.31	3.0
2009	EDH-09-06	N41 58 54.5	W 122 18 58.9	10	55429.45	2527.03	0.23	0.89	8.9
2009	EDH-09-07	N41 58 48.9	W 122 19 36.0	1.8	52387.33	2574.27	0.10	0.31	3.1

Beginning with the downstream end of the reservoir equivalent to zero and the upstream extent of the reservoir equivalent to one, a relative station was calculated for each sample. In addition, relative depth with respect to each station was calculated by setting the minimum bed = 1 and the highest elevation in the cross section = 0. The following function (equation 1) was fit to the data:

$$D = \left(a - bX^{c}\right)Y^{d}$$

where, D = sediment depth

X = relative stationing along reservoir

Y = relative depth within cross section

Constants: $a = 10.35$, $b = 1.69$, $c = d = 1$

For Copco Reservoir, the relationship yields an R^2 value of 0.84 and a root mean squared error of 1.1. Figure 5-33 shows the predicted sediment depths compared with the measured values. The largest difference between the predicted and measured values is 2 feet. The average difference is 1 foot.

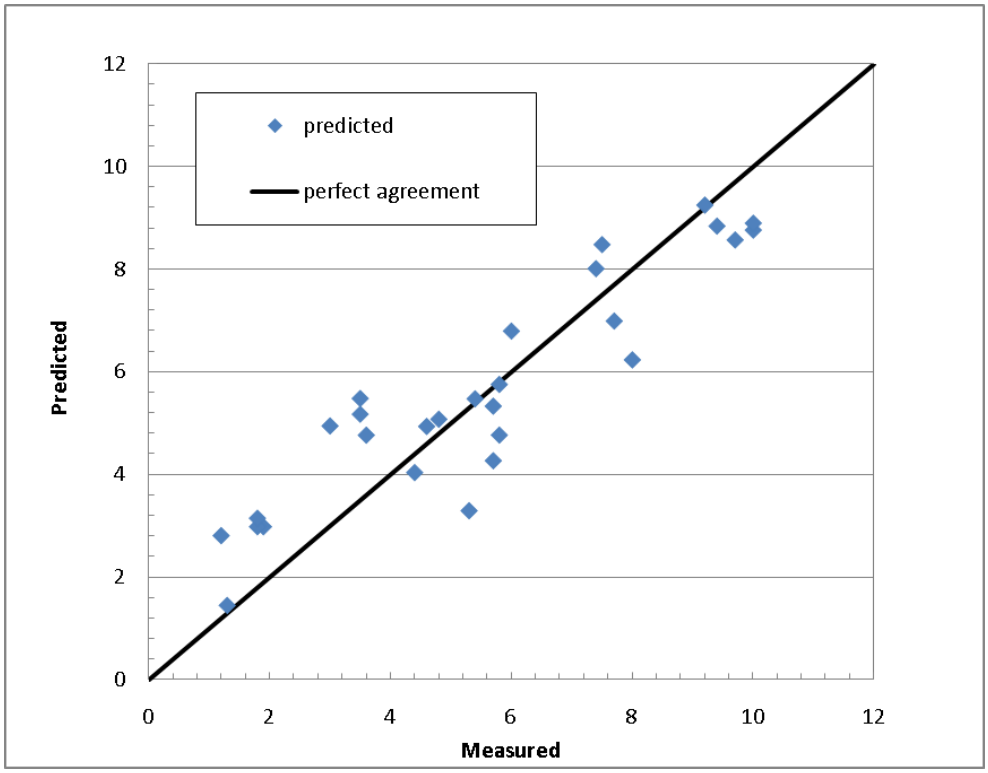

Figure 5-33. Comparison of measured sediment depth to predicted sediment depth from sediment samples collected in 2006 and 2009 in Copco Reservoir.

This relationship was applied to the entire reservoir. The extents were based on the area surveyed by J.C. Headwaters, Inc. (2003). Sediment depths were calculated using ArcMap's (ESRI, Inc.) ArcToolbox raster math functions. Figure 5-36, at the end of this section, shows the map of reservoir thickness and the locations of the 2009 sediment samples. Two areas were modified from the results of the regression function. Any location that produced a negative value was set at zero depth. This occurred in higher elevations around the reservoir edge and at the upstream-most area of the reservoir where sediment depths were higher than anticipated. However, measurements showed that no measureable sediment deposition exists in the upper end of the reservoir and a value of 0.5 feet of sediment as assigned to this area.

The total volume trapped in Copco 1 Reservoir was estimated to be 7.44 million yd^3. An estimate of the uncertainty of this volume was computed by multiplying the average error of the regression equation by the area of the reservoir. This equated to an uncertainty of 1.5 million yd^3, or 20 %.

Iron Gate Reservoir

The method for estimating the sediment depth in Iron Gate Reservoir was similar to that used for Copco 1 Reservoir. A relationship was found between sediment depth and position within the reservoir for collected sediment samples. Samples were measured by Shannon and Wilson (2006) and Reclamation (2009). For Iron Gate Reservoir, 18 samples were used (Table 5-12).

Table 5-12. Sediment sample locations and depths for Iron Gate Reservoir.

Year	Sample Number	Latitude	Longitude	Sediment Depth (ft)	Station (ft)	Bed Elevation (ft)	Relative Station	Relative Bed Elevation	Predicted Sediment Depth (ft)
2006	IG-03	N41 57.659	W122 25.629	2	16397.71	2222.96	0.36	1.02	3.7
2006	IG-04	N41 56.686	W122 25.777	2.5	7967.60	2230.06	0.11	0.72	4.0
2006	IG-05	N41 58.279	W122 22.421	0.5	35186.44	2306.55	0.93	1.24	0.6
2006	IG-07	N41 57.922	W122 25.235	5	18891.26	2232.27	0.44	1.02	3.4
2006	IG-08	N41 57.175	W122 26.039	4.3	11821.86	2198.06	0.23	1.07	4.0
2009	CDH-09-21	N41 58 11.7	W 122 22 26.9	1.5	34906.10	2311.01	0.92	0.58	0.6
2009	CDH-09-22	N41 58 01.7	W 122 23 27.6	1.4	29859.70	2271.78	0.77	1.09	1.8
2009	CDH-09-25	N41 57.820	W 122 25.440	5	17784.95	2235.39	0.40	1.02	3.6
2009	CDH-09-26	N41 57 36.9	W 122 25 26.8	2	17145.91	2283.76	0.39	0.29	3.1
2009	CDH-09-29	N41 57.262	W 122 26.006	4.8	12625.61	2237.78	0.25	0.77	3.8
2009	CDH-09-30	N41 56 50.8	W 122 25 54.6	2.9	9362.28	2193.36	0.15	0.98	4.1
2009	CDH-09-31	N41 56 39.7	W 122 26 12.5	4.8	7908.78	2263.37	0.11	0.37	3.7
2009	CDH-09-32	N41 56.396	W 122 25.882	4.3	6096.50	2216.72	0.05	0.85	4.1
2009	EDH-09-08	N41 58 03.4	W 122 23 21.1	0.3	30369.34	2282.99	0.78	0.91	1.6
2009	EDH-09-08A	N41 58 02.6	W 122 23 41.3	2.2	28775.45	2273.18	0.73	1.10	2.0
2009	EDH-09-09	N41 57 43.0	W 122 25 27.0	2	17435.53	2304.61	0.39	0.24	3.0
2009	EDH-09-09A	N41 57 43.0	W 122 25 30.0	3.8	17226.94	2280.93	0.39	0.24	3.0
2009	EDH-09-10	N41 57 14.5	W 122 25 58.6	4.5	12356.84	2251.67	0.24	0.54	3.7

The same function (equation 1) was used to fit the data at Iron Gate Reservoir. The best fit values for the constants are: $a = b = 4.208$, $c = 2.046$, $d = 0.125$. The relationship yields an R^2 value of 0.54 and a root mean squared error of 1.0. Figure 5-34 shows the predicted sediment depths compared with the measured values. The largest difference between the predicted and measured values is 1.7 feet. The average difference is 0.9 feet.

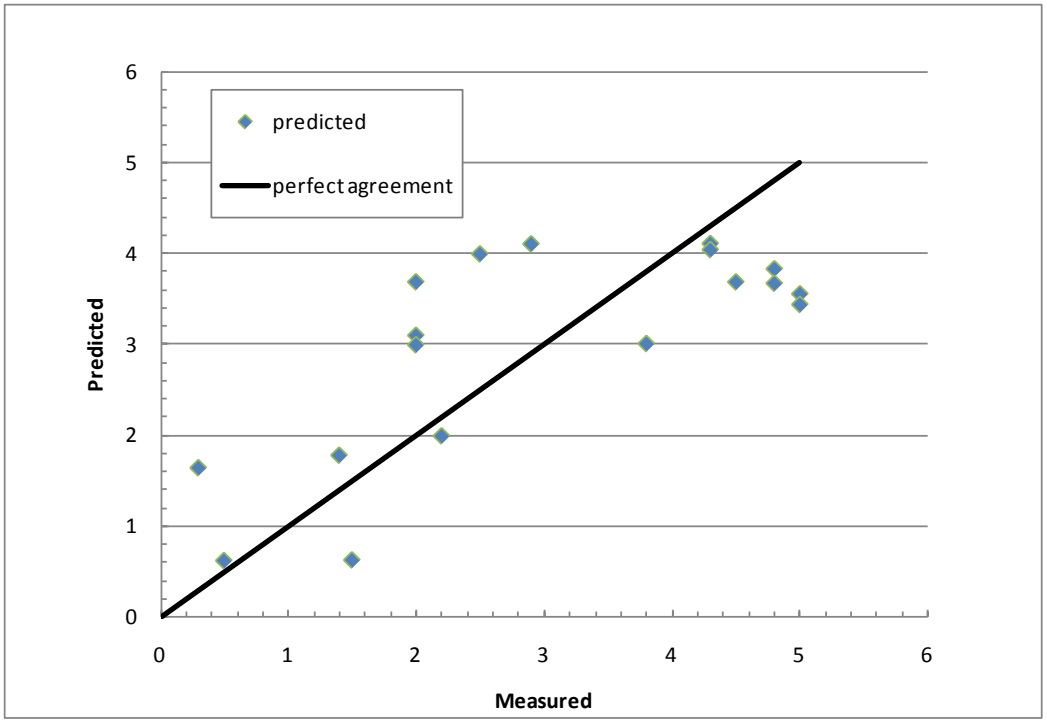

Figure 5-34. Comparison of measured sediment depth to predicted sediment depth from sediment samples collected in 2006 and 2009 in Iron Gate Reservoir.

This relationship was applied to the entire reservoir (the extents were based on the area surveyed by J.C. Headwaters, Inc. (2003). Sediment depths were calculated using ArcMap's (ESRI, Inc.) ArcToolbox raster math functions.

Figure 5-37, at the end of this section, shows the map of reservoir thickness and the locations of the 2009 sediment samples. Three areas were modified from the results of the regression function. Any location that produced a negative value was set at zero depth. This occurred in higher elevations around the reservoir edge. The other two areas were where tributaries enter into Iron Gate Reservoir from the north and influence the sediment deposition. Sediment samples collected in each of these areas were averaged and applied over the approximate area of influence. Jenny Creek is the tributary that enters from the north-east. The average sediment thickness was 6.0 feet. Scotch Creek and Camp Creek enter the reservoir from the north-west. The average sediment thickness in this area is 3.0 feet. See Table 5-13.

The total volume trapped in Iron Gate Reservoir was estimated to be 4.71 million yd^3. An estimate of the uncertainty of this volume was computed by multiplying the average error of the regression equation by the area of the reservoir. This equated to an uncertainty of 1.3 million yd^3 or 29 % (Tables 5-14 and 5-15).

Table 5-13. Sediment samples used to calculate the average thickness where Jenny Creek, Scotch Creek and Camp Creek enter Iron Gate Reservoir.

Year	Sample Number	Latitude	Longitude	Sediment Depth (ft)	Station (ft)	Bed Elevation (ft)
Jenny Creek						
2006	IG-1	N41 58.46	W122 24.001	7.0	26498.02	2306.00
2006	IG-9	N41 58.329	W122 24.277	6.5	25385.74	2270.00
2009	CDH-09-23	N41 58 23.3	W 122 24 05.5	9.2	26138.66	2298.70
2009	CDH-09-24	N41 58 18.6	W 122 24 12.7	4.1	25738.82	2282.40
2009	EDH-09-11	N41 58 17.3	W 122 24 10.9	3.1	25911.94	2281.60
			Average Depth	**6.0**		
Scotch Creek and Camp Creek						
2006	IG-2	N41 57.819	W122 26.16	1.9	14663.72	2254.00
2006	IG-6	N41 58.216	W122 26.255	2.0	17480.57	2299.00
2009	CDH-09-Add 1	N41 57 55.6	W 122 26 07.4	2.4	16822.33	2266.80
2009	CDH-09-27	N41 57 55.8	W 122 26 06.1	4.2	16887.17	2272.40
2009	CDH-09-28	N41 57 47.4	W 122 26 21.2	4.4	14321.23	2290.20
2009	EDH-09-091	N41 57 55.6	W 122 26 07.4	3.0	16822.33	2267.60
			Average Depth	**3.0**		

Table 5-14. Estimated reservoir volumes based upon drill holes.

Reservoir	# holes 2006	# holes 2009	# holes Total	Estimated Volume (yd^3)	Estimated Uncertainty (+/- yd^3)
JC Boyle	5	26	31	990,000	300,000
Copco I	12	17	29	7,440,000	1,500,000
Copco II	0	0	0	0	
Iron Gate	9	19	28	4,710,000	1,300,000

Table 5-15. Average reservoir physical characteristics based upon drill holes.

Reservoir	Location	Volume (yd^3)	Silt and Clay (%)	Water Content (%)	Porosity (-)	Dry Bulk Density (lb/ft^3)	Estimated Dry Weight (tons)
JC Boyle	Upper	380,000	44	172	0.82	29.5	151,000
	Lower	620,000	88	344	0.90	16.3	136,000
Copco I	Upper	810,000	73	287	0.88	19.2	210,000
	Lower	6,630,000	88	295	0.88	18.7	1,674,000
Iron Gate	Upper	830,000	78	192	0.83	27.0	303,000
	Lower	2,780,000	86	276	0.88	19.8	743,000
	Upper Trib	300,000	75	102	0.73	44.4	180,000
	Lower Trib	800,000	94	284	0.88	19.3	208,000
All		**13,150,000**	**84.8**	**278**	**0.87**	**20.3**	**3,605,000**

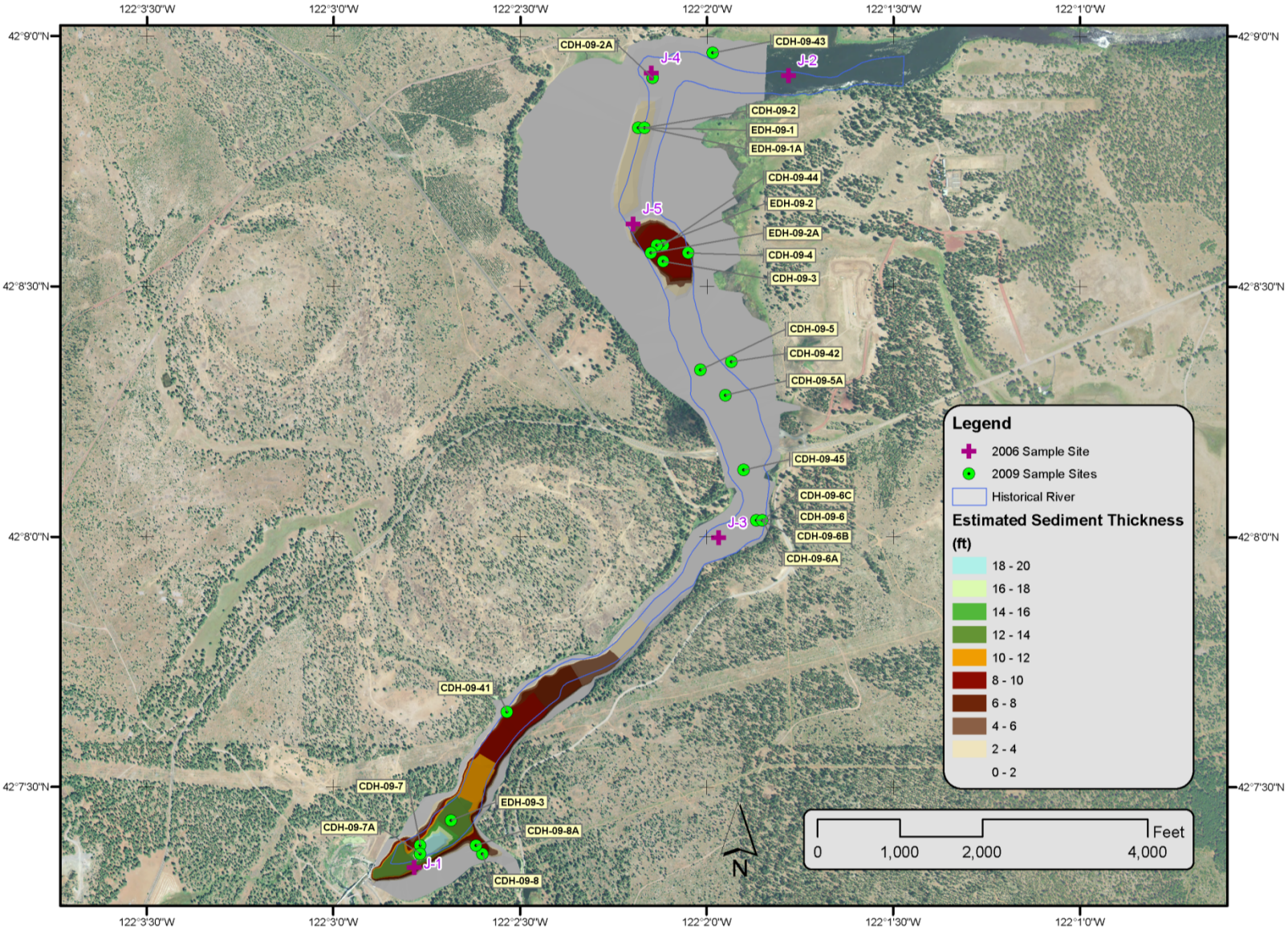

Figure 5-35. J.C. Boyle Reservoir estimated sediment thickness and sample site locations.

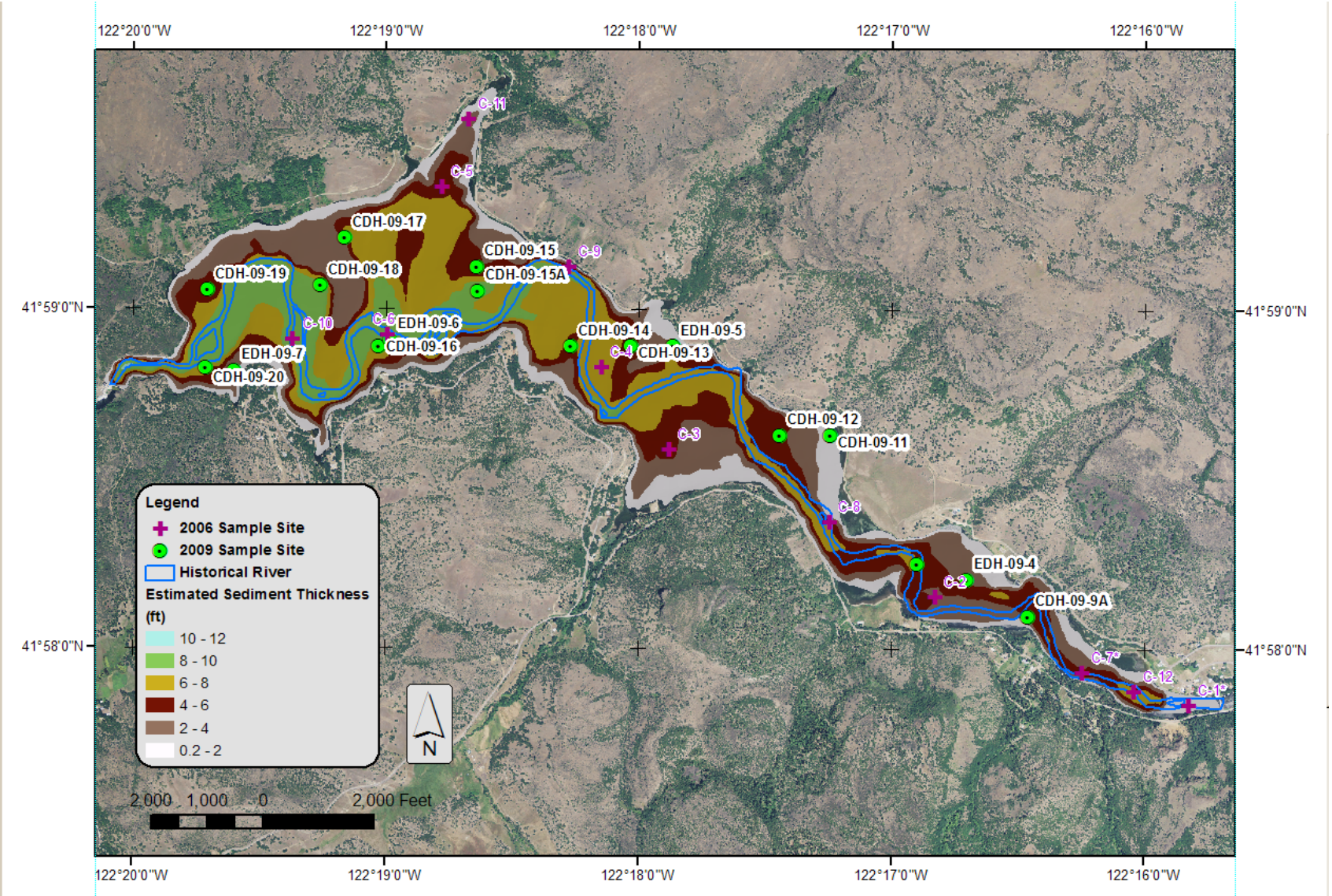

Figure 5-36. Copco 1 Reservoir estimated sediment thickness and sample site locations.

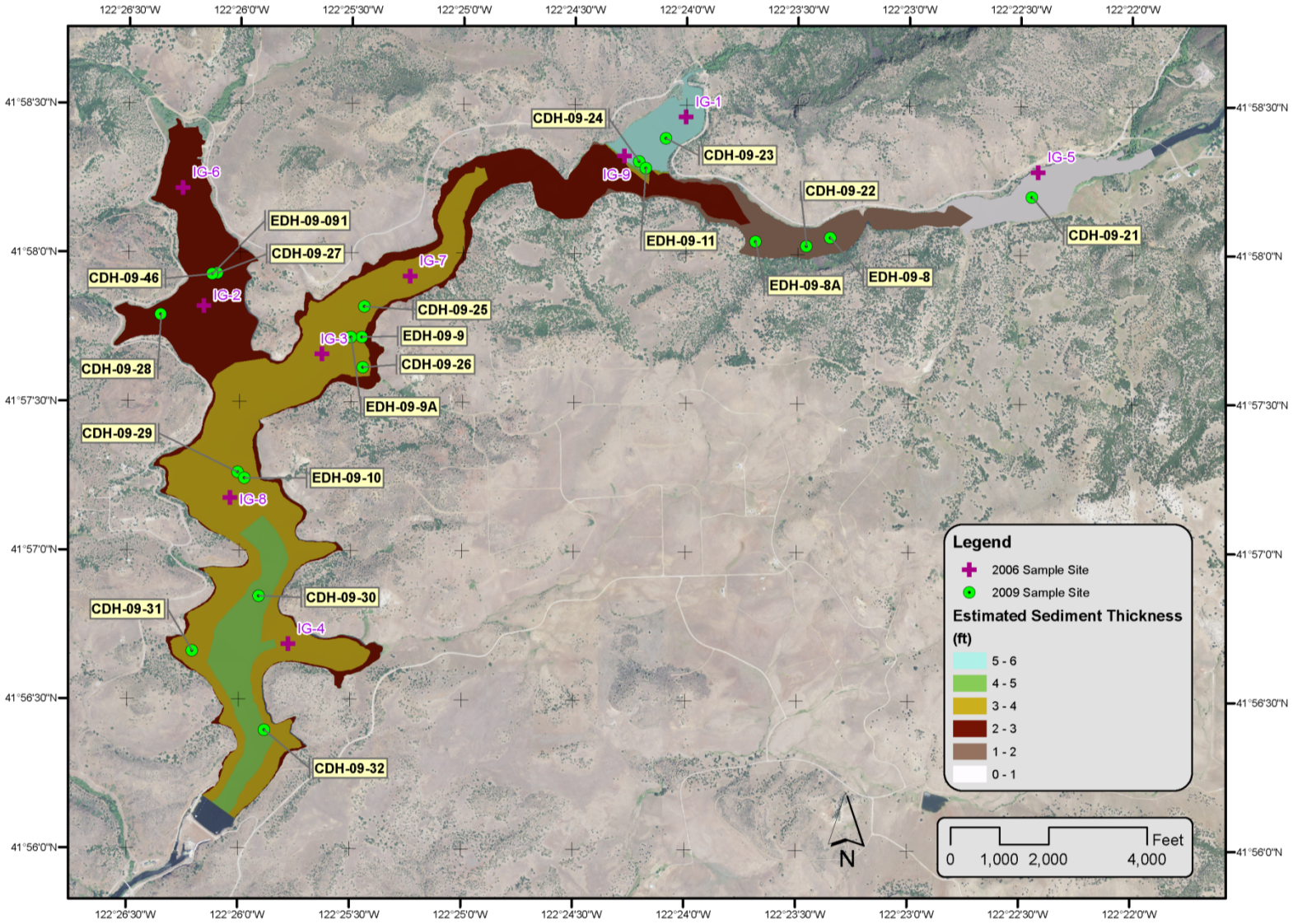

Figure 5-37. Iron Gate Reservoir estimated sediment thickness and sample site locations.

5.6.2. PHYSICAL PROPERTIES

Physical properties such as particle size, bulk density, and water content are important to defining the behavior of the reservoir sediment after dam removal. A particle size and basic engineering properties analyses were conducted on samples from each drill hole and details of the drilling investigation and laboratory analysis are given in Reclamation (2010). Average properties were computed for the upper and lower sections of each reservoir. In addition, the pre-reservoir sediment was averaged separately. At Iron Gate, the samples in the tributary arms were also averaged separately. The separation between upper and lower sections at J.C. Boyle Reservoir was between holes CDH-9-41 and CDH-9-6. At Copco 1 Reservoir, it was between samples CDH-9-11 and CDH-9-10 and at Iron Gate Reservoir, it was between samples CDH-9-25 and CDH-9-24. Results are summarized in Table 5-16.

To calculate the porosity, ε, of the sample the following equation was used:

$$\varepsilon = \left(1 + \frac{1}{\omega s}\right)^{-1}$$

Where ω = water content by mass and *s* = specific gravity of sediment. The dry bulk density of the sediment is

$$\rho_b = \gamma s(1 - \varepsilon)$$

There were two samples classified as MH (Elastic silt) that were tested for specific gravity (*s*). The specific gravity of the material was 2.67 and 2.52, for an average specific gravity of 2.6 (Strauss, 2010).

Table 5-16. Average physical properties of reservoir sediment.

	#	Clay	Silt	Sand	Gravel	LL	PL	WC	η	ρ_d
		%	%	%	%	%	%	%	%	lb/ft^3
JC Boyle										
Upper Reservoir	12	17.3	26.2	56.5	0.0	45.5	14.7	173	0.82	29.5
Lower Reservoir	17	38.2	49.7	12.1	0.0	173	60.6	345	0.90	16.3
Pre-reservoir	2	3.7	9.5	28.4	58.5	44.9	12.7	23.4	0.38	101
Copco 1										
Upper Reservoir	4	27.9	46.8	25.1	0.2	109.3	49.3	287	0.88	19.2
Lower Reservoir	17	55.8	34.2	10.0	0.0	154.3	59.1	295	0.88	18.7
Pre-reservoir	6	35.6	42.2	22.2	0.0	105.0	41.5	153	0.80	32.6
Iron Gate										
Upper Reservoir	7	35.4	43.1	21.6	0.0	70.9	29.9	192	0.83	27.0
Lower Reservoir	10	60.7	25.5	13.5	0.4	118.7	51.4	276	0.88	19.8
Pre-reservoir	8	33.6	16.9	20.4	29.1	60.6	32.5	37.9	0.50	81.8
Upper Tributary	7	31.8	42.7	25.5	0.0	60.7	22.7	102	0.73	44.4
Lower Tributary	6	61.8	32.0	6.1	0.0	112.2	49.6	284	0.88	19.3

Clay = 0 to 0.005 mm
Silt = 0.005 to 0.075 mm
Sand = #200 to # 4 sieve
Gravel = #4 to 3 inch
LL = Liquid limit
PL = Plasticity Index
ω = Moisture Content = Weight Water / Weight Solids
η = porosity
ρ_d = dry bulk density

5.6.3. COHESION AND SHEAR STRENGTH

The shear strength of the reservoir sediment will be important to understanding the behavior of the sediment upon drawdown. Sediment with low shear strength will slump downslope as it will be unable to resist the force of gravity. The shear strength of the sediment can be computed as:

$$\tau_f = c' + (\sigma - \mu_w)\tan\phi'$$

where, τ_f = soil shear stress

c' = effective cohesion
σ = normal stress
μ_w = pore water pressure
ϕ' = effective angle of internal friction

Strauss (2010) performed direct shear tests on three drill core samples taken from each reservoir, holes EDH-9-3, EDH-9-6, and EDH-9-9A. The measured friction angles (ϕ') were 29.8º, 27.3º and 32.3º, respectively. The measured cohesion values (c') were 1.1, 0.8, and 0.7 lbf/in^2. Because the material is so soft, it was difficult to obtain accurate estimates of its shear strength and Strauss (2010) stated that actually shear strength may be less than measured.

If is possible to calculate the stable depth of an section of the deposit assuming infinite slope using the US Army Corps of Engineers Slope Stability Engineering Manual (EM-1110-2-1902, USACOE, 2003). The analysis is described in Appendix E of the manual and assumes that the soil rests on top of a firm base. It accounts for seepage. Table 5-17 contains the estimated stable depth of reservoir sediment assuming different values of the cohesion and different slope values. It is assumed that the sediment is fully saturated and draining. As a conservative assumption, it was assumed that the minimum effective cohesion value would be 50 % of the minimum measured value or 0.35 lbf/in^2. Therefore, on a slope of 10%, the stable depth is over 8 feet, which would encompass all of the sediment in Iron Gate and the most all of the off-channel sediment in Copco and J.C. Boyle.

Table 5-17. Stable depth of reservoir sediment assuming infinite slope and that the sediment is fully saturated. The minimum measured cohesion value was 0.7 lbf/in^2.

Slope	**Stable Depth for Different *c'* values**			
	***c'* (lbf/in^2)**			
	0.2	**0.35**	**0.7**	**1**
0.1	4.6	8.1	16.2	23.1
0.2	2.4	4.2	8.3	11.9
0.3	1.7	2.9	5.8	8.3
0.4	1.3	2.3	4.7	6.7

5.6.4. EROSIVE PROPERTIES

The most common equation used to predict the erosion of cohesive sediment erosion is:

$$E = k_d(\tau - \tau_c)$$

where E = erosion rate,
k_d = erosion rate constant,
τ = shear stress, and
τ_c = critical shear stress.

There were two sets of tests on the sediment. One set of tests was on samples from 3.5 inch acrylic tube samples. These samples were collected as part of the geological investigation described in Strauss (2010). These were analyzed by the Bureau of Reclamation in Denver, CO. The measured results of the jet tests on the drill cores are given in Appendix C. Jet Test Results from TSC and shown Figure 5-40.

Another set of samples were collected by a 9-inch Ponar sampler. These samples were repacked in the lab and tested using a jet test device described in Simons et al. (2010). The sample collected from the Ponar sampler is shown in Figure 5-38 and the sampling device is shown in Figure 5-39. The description of the testing procedure is given in Appendix D. Report on Erodibility Characteristics of Reservoir Sediment by Agricultural Research Service. The results are shown in Figure 5-41 and summary statistics are given in Table 5-18. Samples were tested under wet and dry conditions. The effects of drying on erosion resistance and erodibility (τ_c and k_d) were significant with reservoir-average values of τ_c increasing by at least an order of magnitude. Associated decreases in k_d also occurred with sample drying, but not to the extent of the increases in critical shear stress. The median value of the erodibility coefficient decreased by about 80%. The average erodibility of the moist reservoir sediment was similar to that of sand, while the average erodibility of the dried sediment was similar to that of gravel or cobbles.

Simulations of the sediment used the 25th, 50th, and 75th Percentiles of τ_c and k_d.

Table 5-18. Summary of jet tests on sediment from all reservoirs from Simons et al. (2010).

	τ_c (Pa)	k_d (cm^3/N-s)
Moist Sample		
Minimum	0.000	0.23
25th Percentile	0.032	0.57
50th Percentile	0.21	0.82
75th Percentile	1.18	1.23
Max	4.83	5.6
Average	0.94	1.4
Dry Samples		
Minimum	1.2	0.04
25th Percentile	2.7	0.12
50th Percentile	5.9	0.16
75th Percentile	17.8	0.32
Max	113.6	0.59
Average	24.7	0.23

Figure 5-38. Sample just after release from Ponar sampling device.

Figure 5-39. Ponar sampling device used to collected disturbed samples.

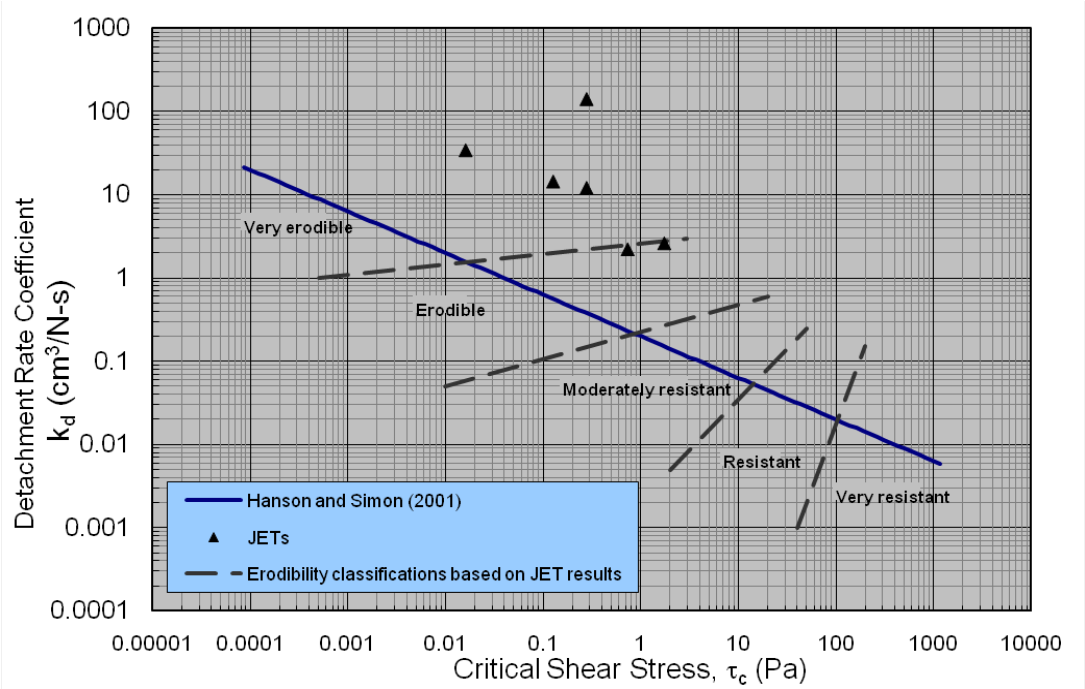

Figure 5-40. Results from jet tests on drill core samples. Details in Appendix C. Jet Test Results from TSC.

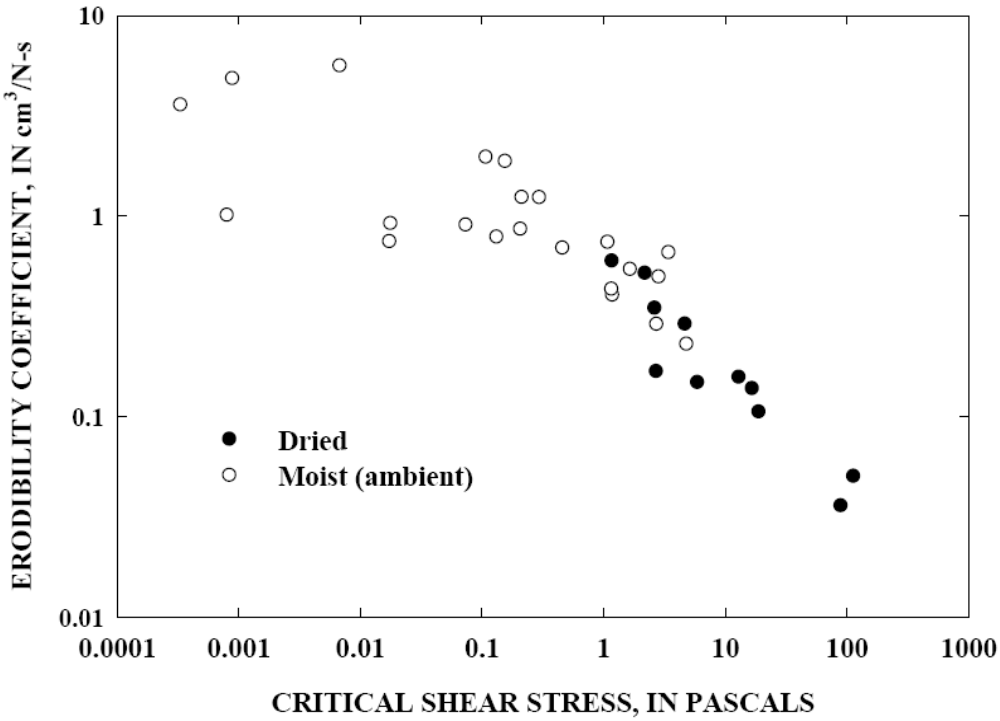

Figure 5-41. Measured critical shear stress (τ_c) and erodibility coefficient (k_d) for moist and dried samples (From Simon et al. 2010).

5.6.5. CONSOLIDATION AND DESICCATION

The sediment is primarily water with an average water content of over 80% by volume. After the reservoir is drawn down, the sediment will dry and decrease in thickness. A simple test of the sediment consolidation was performed by placing wet sediment into free draining plastic containers. Holes were cut into the bottom of the container and gravel placed on the bottom so that the sample could drain freely. The sample was allowed to dry outside, uncovered and exposed to the elements. The initial and final depths of the sample are given in Table 5-19. The desiccated depth of the sample was about 60% of the initial depth. In addition, deep cracks developed in the soil and the sampled pulled away from the container edges. We estimate that the volume of the sample decreased by approximately 66%. The porosity changed from 0.82 to approximately 0.46. The bulk density increased from 29.5 lb/ft^3 to approximately 87 lb/ft^3. The sample tested was taken from the upper portion of J.C. Boyle Reservoir and has a slightly higher bulk density than the sediment in the lower portions of the three reservoirs. The dry bulk density of the finer sediment located in the lower parts of the three reservoirs is expected to increase from its existing value of 16 – 20 lb/ft^3 to between 47 to 58 lb/ft^3.

Table 5-19. Change in depth of reservoir sediment after desiccated in an open air and freely draining container.

Container	Initial Depth (in)	Final Depth (in)	% of original depth
1	7.00	4.25	60
2	7.88	4.63	59
3	4.50	2.75	61

Figure 5-42. Picture of sediment from J.C. Boyle Reservoir immediately after placement.

Figure 5-43. Picture of sediment from J.C. Boyle Reservoir 15 days after placement.

5.6.6. FALL VELOCITY

The fall velocity of the sediment is important to defining the rate at which particles will settle in the riverine or reservoir environment. General relationships for fall velocity are available for non-cohesive sediment, which is generally defined as sediment with particle diameter greater than 62 µm (Mehta and Mcanally, 2008). The influence of cohesive forces relative to gravity forces generally increases with decreasing particle size, and when particles are 2 µm or less, cohesive forces will dominate (Mehta and Mcanally, 2008).

In the lower portion of Iron Gate Reservoir and Copco Reservoir where the bulk of the sediment is located, over 50% of the particles have diameters less than 5 µm and therefore cohesive forces will be important to the characteristics of the particles behavior. Deas et al (2010) collected samples of the sediment contained in the water column at one site upstream of Copco Reservoir, three sites within Copco Reservoir and one site downstream of Iron Gate Dam. The samples were taken to a lab where the fall velocity of the particles where measured with a Laser In-Situ Scattering and Transmissometry with Settling Tube (LISST-ST) in a bench top setting. The LISST-ST measures the settling rates and particle size distribution of the samples. The mean settling rate of the sediment sampled from the reservoir sites was 0.55 m/d and the average for the river sites was 2.7 m/d. The detention time of Copco and Iron Gate reservoirs under average flow conditions is 12 and 16 days (PacifiCorp, 2004). The ratio of annual inflow to storage volume for the reservoirs is 0.033 and 0.044. Based upon the Brune (1953) curve for fine-grained as modified by Morris and Fan (1998), the trap efficiency of the reservoirs would approximately about 60% at Copco Reservoir and about 70% Iron Gate Reservoir. The trap efficiency can also be based upon the methods used in Pemberton and Lara (1971) for settling basins:

$$\text{Trap Efficiency} = 1 - \exp\left(-\frac{lw_f}{Vd}\right)$$

where l = length of basin
w_f = fall velocity
V = average flow velocity
D = basin depth

Rearranging the equation gives:

$$\text{Trap Efficiency} = 1 - \exp\left(-\frac{Aw_f}{Q}\right)$$

where A = plan area of basin
w_f = fall velocity
Q = flow rate through basin

Using the fall velocity of 0.55 m/d and an average flow rate of 1885 cfs gives a trap efficiency of approximately 45% at Copco and Iron Gate reservoirs. Based upon these analyses, trap efficiencies of 50 to 75% are expected for each reservoir. The effective trap efficiencies of the reservoir in series would be between 75% and 94%.

The settling rate of particles can also depend upon the concentration (Figure 5-44). A study by Van Rijn (1993) using data collected in various rivers and estuaries concluded that the settling rates of sediment at a concentration of 1,000 to 10,000 mg/l can be an order of magnitude greater than the settling rates of sediment at a concentration of less than 100 mg/l. This is because cohesive sediment particles will tend to flocculate at higher concentrations and increase their diameter and settling velocity. As the concentrations exceeds around 10,000 mg/l, the concentration of particles is high enough to prevent settling because the particles basically run into each other and cannot settle.

The concentrations were not reported by Deas et al (2010), but the samples were collected during a period of relatively low flow and therefore the concentrations were most likely less than 100 mg/l. Therefore, the settling rates during periods of high concentration could be significantly higher.

Table 5-20. Measured settling rates from Table 2 of Deas et al (2010).

Table 2. Settling rates and standard deviations of settling rates for samples at river and reservoir sites.

		Settling Rate, meters per day								
Date and Time	Site	3.48 microns	6.76 microns	13.12 microns	25.48 microns	49.4 microns	95.82 microns	185.82 microns	360.34 microns	*Site Standard Deviation*
	River sites									
8/12/2008 13:30	KR above Shovel Creek - 8/12	0.20	0.17	0.55	1.08	3.07	6.70	1.18	0.17	*2.26*
8/14/2008 12:25	KR above Shovel Creek - 8/14	0.20	0.17	0.73	1.43	5.51	12	12	0.93	*5.16*
8/14/2008 14:00	KR at Klamathon	0.19	0.17	0.47	0.82	2.5	5.51	8.14	1.82	*2.90*
	Average	*0.20*	*0.17*	*0.58*	*1.11*	*3.69*	*8.08*	*7.11*	*0.97*	
	Standard Deviation	*0.01*	*0.00*	*0.13*	*0.31*	*1.60*	*3.47*	*5.49*	*0.83*	
	Standard Deviation / Average	*3%*	*0%*	*23%*	*28%*	*43%*	*43%*	*77%*	*85%*	
	Reservoir sites									
8/12/2008 12:35	KR near Copco Bridge	0.17	0.39	0.41	0.55	1.0	1.6	0.35	0.17	*0.49*
8/11/2008 7:30	Copco Mid Reservoir	0.17	0.17	0.47	0.93	1.6	0.32	0.31	0.60	*0.49*
8/14/2008 7:30	Copco near Dam	0.19	0.17	0.51	0.93	1.43	0.47	0.17	0.17	*0.46*
	Average	*0.18*	*0.24*	*0.46*	*0.80*	*1.34*	*0.80*	*0.28*	*0.31*	
	Standard Deviation	*0.01*	*0.13*	*0.05*	*0.22*	*0.31*	*0.70*	*0.09*	*0.25*	
	Standard Deviation / Average	*7%*	*52%*	*11%*	*27%*	*23%*	*88%*	*34%*	*79%*	

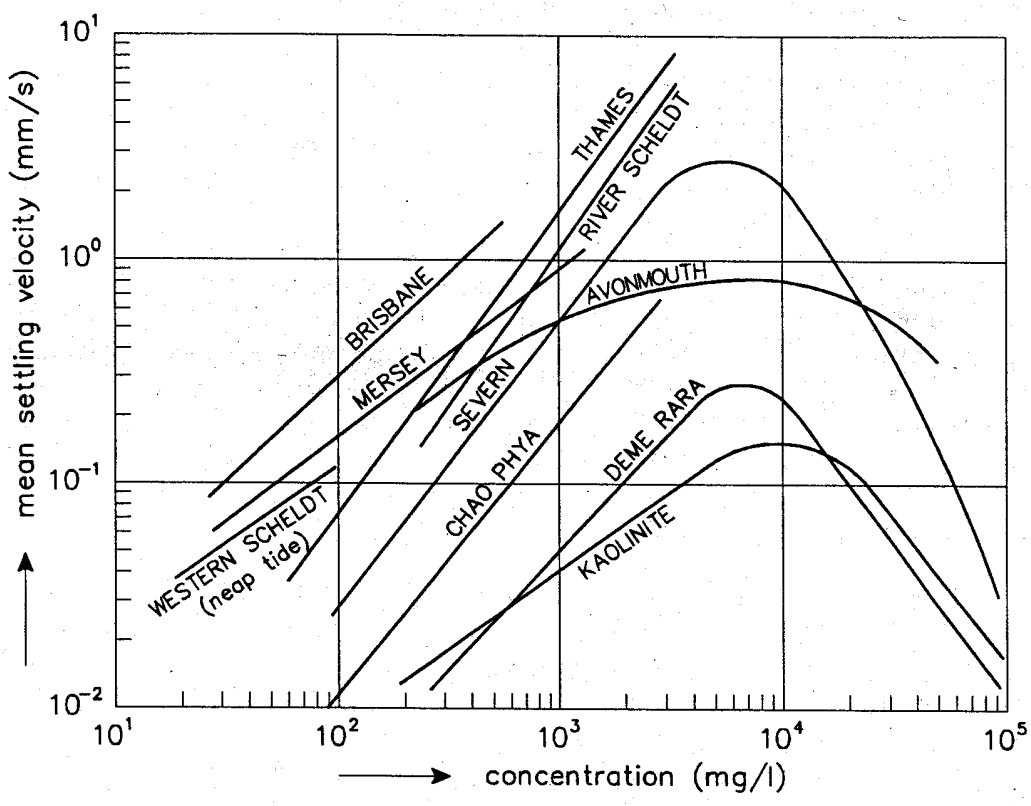

Figure 5-44. The influence of sediment concentration on the settling velocity for various rivers and estuaries (source: Van Rijn, 1993, figure 11.4.2).

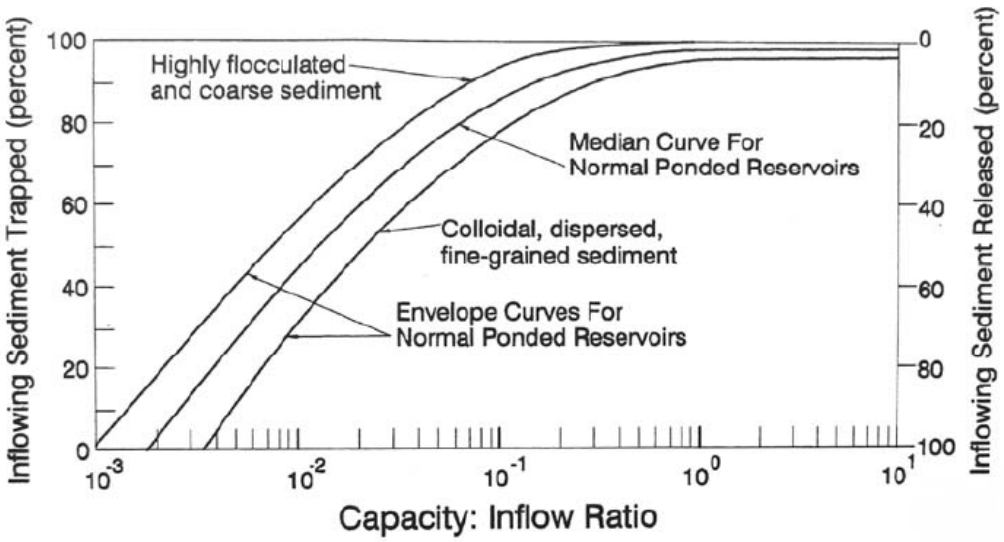

Figure 5-45. Trap efficiency for reservoirs (source: Morris and Fan, 1998, Figure 10.15).